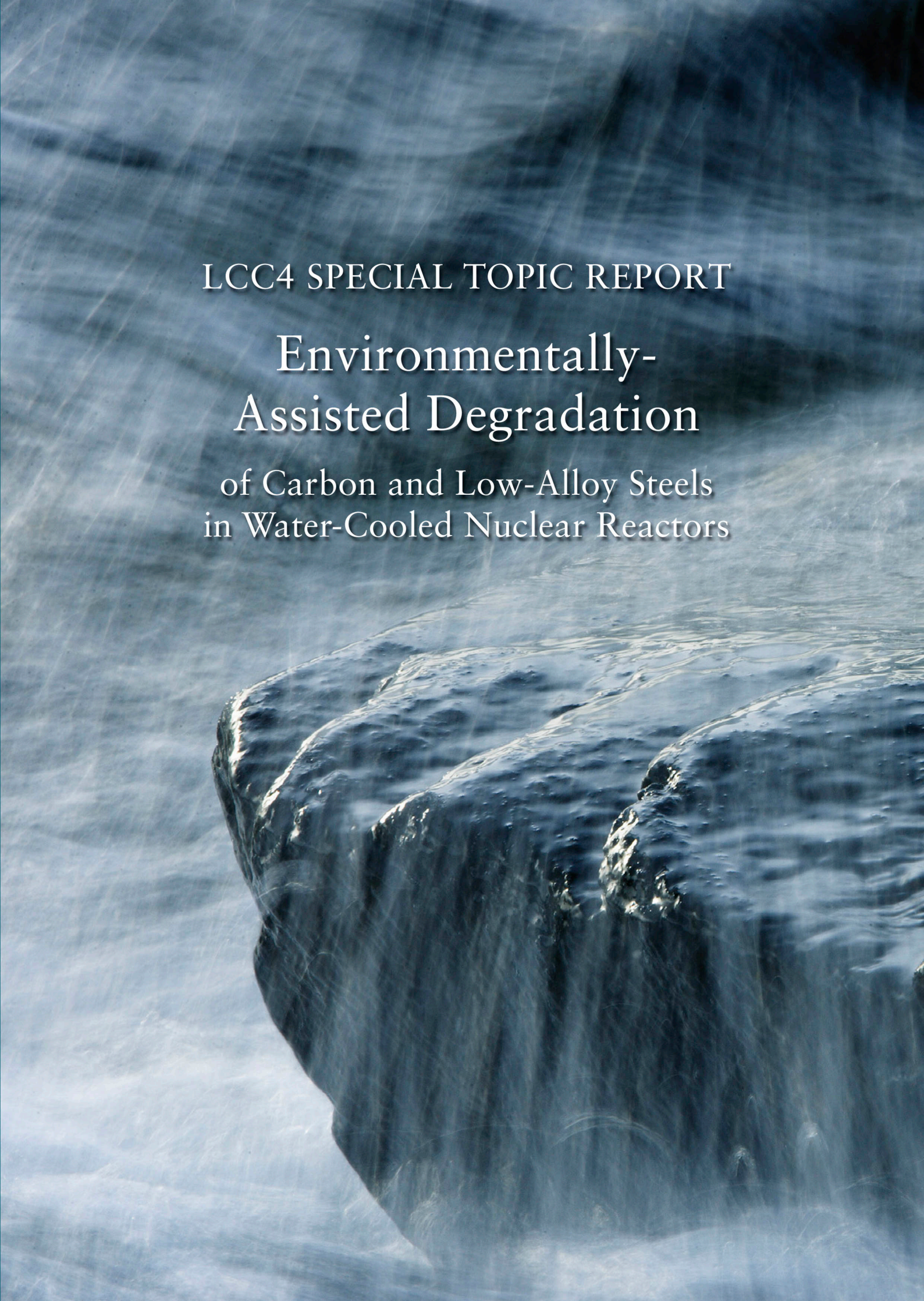

LCC4 SPECIAL TOPIC REPORT

Environmentally-Assisted Degradation

of Carbon and Low-Alloy Steels in Water-Cooled Nuclear Reactors

Environmentally-Assisted Degradation of Carbon and Low-Alloy Steels in Water-Cooled Nuclear Reactors

Authors

F. Peter Ford
Rexford, NY 12148, USA

Peter M. Scott
Noisy-Le-Roi, France

A.N.T. INTERNATIONAL®

Advanced Nuclear Technology International
Krongjutarvägen 2C, SE-730 50 Skultuna
Sweden

info@antinternational.com
www.antinternational.com

Disclaimer

The information presented in this report has been compiled and analysed by Advanced Nuclear Technology International Europe AB (ANT International®) and its subcontractors. ANT International has exercised due diligence in this work, but does not warrant the accuracy or completeness of the information. ANT International does not assume any responsibility for any consequences as a result of the use of the information for any party, except a warranty for reasonable technical skill, which is limited to the amount paid for this assignment by each *LCC4* programme member.

Acronyms and expressions

ASME	American Society of Mechanical Engineers
ASTM	American Society for Testing Materials
AVT	All Volatile (Chemical) Treatment
BAC	Boric Acid Corrosion
BMI	Bottom Mounted Instrumentation (nozzles)
BWR	Boiling Water Reactor
BZT	Benzotriazole
C&LAS	Carbon and Low Alloy Steels
CCT	Continuous – Cooling –Transformation (Diagram)
CCW	Closed Cooling Water (System)
CDF	Core Damage Frequency
CERL	Central Electricity Research Laboratories
CF	Corrosion Fatigue
CFR	Code of Federal Regulations
CGR	Crack Growth Rate
CUF	Cumulative Usage Factor
CR	Corrosion Rate
CRDM	Control Rod Drive Mechanism
CRUD	Chalk River Unidentified Deposit (or English slang term for "dirt")
CST	Condensate Storage Tank
CT	Compact Tension (design of stress corrosion and corrosion fatigue test specimen)
CVCS	Chemical and Volume Control System
CZR	Central Zone Remelting
DL	Disposition Line (relationship between crack propagation rate and stress intensity factor)
DSA	Dynamic Strain Aging
EAC	Environmentally-Assisted Cracking
ECCS	Emergency Core Cooling System
EDF	Electricite de France
EFPH	Effective Full Power Hours
EFPY	Effective Full Power Years
ESHT	Electroslag Hot Topping
ESR	ElectroSlag Remelting
EPRI	Electric Power Research Institute
FAC	Flow Accelerated Corrosion
GALL	Generic Aging Lessons Learned (Report)
GAO	General Accounting Office (of US Congress)
GL	Generic Letter
GDC	General Design Criteria
HAZ	Heat Affected Zone (adjacent to a weld)
HCF	High Cycle Fatigue
HPI	High Pressure Injection
HWC	Hydrogen Waster Chemistry (for *BWR*s)
ID	Inner Diameter
IGA	Intergranular Attack
IGSCC	Intergranular Stress Corrosion Cracking
KWU	KraftWerkUnion
LCC	*LWR* Coolant Chemistry
LCF	Low Cycle Fatigue
LP	Low Pressure (stages in steam turbine)
LWR	Light Water Reactor
MA	Mill Anneal
MIC	Microbiologically-Influenced Corrosion
M_f	Martensite Finish (Temperature)
M_s	Martensite Start (Temperature)

MSLR	Main Steam Line Radiation
NDE	Non-Destructive Examination
NISA	Nuclear and Industrial Safety Agency (of Japan)
NMCA	Noble Metal Chemical Addition
NRC	Nuclear Regulatory Commission
NWC	Normal Water Chemistry (for *BWR*s)
OD	Outer Diameter
OTSG	Once Through Steam Generator
PWHT	Post Weld Heat Treatment
PWR	Pressurized Water Reactor
PWSCC	Primary Water Stress Corrosion Cracking
RCS	Reactor Coolant System
RPV	Reactor Pressure Vessel
RSG	Recirculating Steam Generator
SCC	Stress Corrosion Cracking
SCCI	Stress Corrosion Cracking Index
SEM	Scanning Electron Microscope
SICC	Strain Induced Corrosion Cracking
SRB	Sulphate Reducing Bacteria
SSRT	Slow Strain Rate Testing (for evaluation of *SCC* susceptibility)
TGSCC	Transgranular Stress Corrosion Cracking
TLAA	Time Limited Aging Analysis
TT	Transition Temperature (for brittle to ductile behaviour in fracture resistance Charpy test
TTA	Tolyltriazole
TTT	Temperature-Time-Transformation (Diagram)
UKAEA	United Kingdom Atomic Energy Authority
UTS	Ultimate Tensile Strength
USNRC	United States Nuclear Regulatory Commission
VVER	Voda Voda Energo Reactor (Russian version of *PWR*)
VHN	Vickers Hardness Number
VIP	Vessel Internals Program (of *EPRI*)
WOL	Wedge Opening Loading (referring to a *SCC* specimen design)

Unit conversion

TEMPERATURE		
°C + 273.15 = K		°C*1.8 +32 = °F
T(K)	T(°C)	T(°F)
273	**0**	32
289	16	61
298	25	77
373	**100**	212
473	**200**	392
573	**300**	572
633	360	680
673	**400**	752
773	**500**	932
783	510	950
793	520	968
823	550	1022
833	560	1040
873	**600**	1112
878	605	1121
893	620	1148
923	650	1202
973	**700**	1292
1023	750	1382
1053	780	1436
1073	**800**	1472
1136	863	1585
1143	870	1598
1173	**900**	1652
1273	**1000**	1832
1343	1070	1958
1478	1204	**2200**

Radioactivity	
1 Sv	= 100 Rem
1 Ci	= 3.7 x 10^{10} Bq = 37 GBq
1 Bq	= 1 s^{-1}

MASS	
kg	lbs
0.454	**1**
1	2.20

DISTANCE	
x (µm)	x (mils)
0.6	0.02
1	0.04
5	0.20
10	0.39
20	0.79
25	0.98
25.4	**1.00**
100	3.94

PRESSURE		
bar	MPa	psi
1	0.1	14
10	**1**	142
70	7	995
70.4	7.04	**1000**
100	10	1421
130	13	1847
155	15.5	2203
704	70.4	**10000**
1000	100	14211

STRESS INTENSITY FACTOR	
MPa√m	ksi√inch
0.91	**1**
1	1.10

Summary

Carbon and low alloy steels are widely used as structural materials in water-cooled reactors because of their satisfactory mechanical properties, ease of fabrication, relatively low cost, and a wide experience base in other industries such as fossil power, petrochemical, gas, etc.

Early concerns specific to the nuclear power industry were associated with general corrosion (and its impact on crud formation), fatigue and irradiation embrittlement; these were addressed at the design stage. However in the intervening years there have been numerous instances of environmentally-assisted degradation in various components in the primary, secondary and tertiary systems in water-cooled reactors. These incidents have ranged from crevice corrosion of carbon steel tube support plates in the *PWR* secondary system, to microbiologically-influenced corrosion in the service water system, to intergranular stress corrosion cracking in *PWR* and *BWR* steam turbine discs and to transgranular stress corrosion cracking in the *BWR RPV* feedwater piping.

These phenomena are discussed in this report in terms of the material, environment and, where applicable, stress conditions that control the degree of degradation observed in both laboratory tests and reactor operations. Such knowledge leads to a definition of sustainable mitigation actions.

Attention is placed on an understanding of the chronology of events that lead to "failure" of a component, and the mechanisms that are relevant in that chronology. This emphasis is made since it offers a skeleton upon which to base an analysis of the sometimes complex interactions between the material, environment and stress drivers.

This report is written at this time with the aim of bringing partial closure on the topic of environmentally-assisted degradation of carbon and low alloy steels in water-cooled reactors, since there is a justifiable viewpoint that the major degradation modes are understood well enough that mitigation and control criteria are in place, and that the risk associated with such degradation modes is acceptably low. Unacceptable events *have* certainly occurred in recent times (for instance, flow assisted corrosion of a steam line leading to pipe rupture at Mihama, and boric acid corrosion through the low alloy steel section of the pressure vessel head at Davis Besse) and these have significantly impacted the public perception of safety of reactor components. However these incidents have been ascribed primarily to lack of management oversight, rather than a lack of technical knowledge of the phenomena.

Contents

1 Introduction

This report is one of a series of topical reports covering environmentally-assisted degradation of structural materials in water-cooled nuclear reactors. The first in the series (Ford, 2006) served as an introduction to the subject, being aimed at personnel who were either new to the topic or needed a "refresher-course"on the underlying principles of uniform and localized corrosion phenomena relevant to the structural materials in water-cooled nuclear reactors. This second report in the series uses the 2006 report as a base and focuses in more detail on the environmentally-assisted degradation of carbon and low–alloy steels due to the aqueous environment[1].

Carbon and low-alloy steels make up a major portion of the materials of construction for pressure retaining components in water-cooled nuclear reactors. The choice of these materials was based on their low cost (in comparison to the higher-alloyed materials such as stainless steels and nickel-base alloys), their good fracture resistance (in the unirradiated condition) and, finally, their ease of fabrication. Moreover there was extensive, satisfactory experience with these alloys from other industries, such as petrochemical and fossil power.

The "American Society of Mechanical Engineers (*ASME*) Boiler and Pressure Vessel Code Section III, Nuclear Power Plant Components" outlines the criteria that must be adhered to for pressure–boundary components. Very similar criteria exist in other nations. These criteria are accepted (with some modifications) by the US Nuclear Regulatory Commission (*USNRC*), with the details outlined in Title10 of the Code of Federal Regulations (*CFR*) Part 50, which addresses the criteria for domestic licensing of light water reactors. In particular, these criteria are discussed in Appendix A of 10*CFR*50, which covers the General Design Criteria (*GDC*), and in 10*CFR*50.55, which addresses the conditions for a construction permit and the associated codes and standards ((10*CFR*50.55a).

The 1977 *ASME* Section III design code followed a relatively conservative philosophy (Roberts, 1981) as illustrated by the following quote from the code;

"The potential failure modes and various stress categories are related to the Code provisions, as follows;

a) The primary stress limits are intended to prevent plastic deformation and to provide a nominal factor of safety on the ductile burst pressure.
b) The primary and secondary stress limits are intended to prevent excessive plastic deformation leading to incremental collapse and to validate the application of elastic analysis when performing the fatigue evaluation.
c) The peak stress limit is intended to prevent fatigue failure as a result of cyclic loading.
d) Special stress limits are provided for elastic and inelastic instability.

Protection against brittle fracture is provided by material selection rather than analysis. ***Protection against environmental effects, such as corrosion and radiation effects, is the responsibility of the designer.***"[2]

Thus, at least in the US, it is apparent that the *ASME* Section III design criteria relevant to the current Light Water Reactor (*LWR*) fleet were driven by mechanical property considerations and the only materials degradation modes considered were general corrosion (in terms of its effect on net section stress), fatigue and embrittlement. A similar situation exists, for instance, in France although recent changes have been made that dictate that all reasonably anticipated degradation modes must be taken into account at the design stage.

[1] The metallurgy of irradiation induced embrittlement of low alloy pressure vessel steels is not included in this report

[2] Bold font inserted by authors.

However, it was recognized by the designers that two unique problems could face carbon and low alloy steels in nuclear reactor operation. First, that irradiation embrittlement of the pressure vessel steel would occur in high neutron flux regions over time and, second, that corrosion products could be irradiated during passage through the core region and, would, thereby, create radioactive Chalk River Unidentified Deposit ("*CRUD*") that could hamper maintenance operations.

Consequently these particular problems were addressed proactively by, for instance, the monitoring of the extent of irradiation embrittlement that was being accrued in archive low alloy steel samples placed adjacent to a reactor pressure vessel wall in the high neutron flux "beltline" region. This measured accrual of embrittlement is assessed by the regulatory bodies and is an input to their decisions when specific reactor owners apply for license renewal (sometimes referred to as "life extension"). The crud/radioactivity issue was addressed by cladding the inside of the reactor pressure vessel with stainless steel, thereby reducing the inventory of corrosion product that could become irradiated.[3]

Finally, the question of fatigue damage was addressed by the *ASME* Section III design code, with some assessment being made in the code of the effect of the environment[4] on the fatigue life of components subject to various extents of cyclic loading; this aspect is addressed in some detail in Section 5.4.4.

Thus it was on the basis of cost, satisfactory experience in other industries, and the proactive assessment and control of the specific issues of irradiation embrittlement, radioactive *CRUD* formation and fatigue, that carbon and low-alloy steels have found wide usage in water-cooled reactors in the primary, secondary and tertiary systems in both Boiling Water Reactor (*BWR*) and Pressurized Water Reactors (*PWR*).

In spite of this reasoning, environmentally-assisted degradation has been observed in critical components of *LWR* by degradation modes that were not fully assessed at the design stage. These modes include, for instance,

- "High-cycle" (i.e. low strain amplitude/high frequency) fatigue due to flow induced vibration or thermal stress cycles in e.g. dead legs and feedwater nozzles.
- "Low-cycle" (i.e. high strain amplitude/low frequency) fatigue due to e.g. start-up-shut down cycles.
- Pitting of carbon steel components, usually under oxidizing conditions at lower temperatures, which often acts as a precursor to Stress Corrosion Cracking (*SCC*) during subsequent operation at higher temperatures.
- Transgranular Stress Corrosion Cracking (*TGSCC*) of e.g. *BWR* carbon steel piping and low alloy steel *PWR* steam generator shells, in situations involving dynamic loading, oxidizing environments and high yield stress.
- Intergranular Stress Corrosion Cracking (*IGSCC*) at elevated temperatures of components such as *PWR* steam generator inlet piping that had been cold formed.
- *IGSCC* of welded carbon steel piping in lower-temperature, Closed Cooling Water (*CCW*) systems containing inhibitors, and in low alloy steel steam turbine components operating at temperature/pressure combinations associated with the Wilson line[5].
- Microbiologically-Influenced Corrosion (*MIC*) of carbon steel piping in tertiary systems such as the service-water and fire suppression systems.
- Flow-Accelerated Corrosion (*FAC*) of carbon steel components in, for instance, the *PWR* steam generator tube support plates, secondary feedwater and steam/condensate piping, and in *BWR* feedwater, main steam line and auxiliary systems.

---

[3] There is a school of thought that it is better to accept the higher crud release from carbon and low alloy steels rather than the lower amount from stainless alloys because the activation products of the former are less energetic and shorter lived. This philosophy was accepted by CANDU and the early VVERs.

[4] Note that the "environment" considered in the development of the *ASME* Section III design curves was an "industrial environment", not a specific water-cooled reactor environment.

[5] The Wilson line corresponds to the pressure/temperature conditions in the turbine where 1-3% moisture exists in the equilibrium steam/condensate mixture

- Boric Acid Corrosion (*BAC*) of low alloy steel components adjacent to leaks in the *PWR* primary system.
- Hydrogen embrittlement of high strength martensitic and maraging low alloy steel bolting largely used in air environments (e.g. vessel head, pump casings).

These incidences have been reported in conferences that have focused on the degradation of materials in water-cooled reactors (Environmental Degradation Conferences, 1983-2007) and in publications from, for instance, the *USNRC* on their website (http://www.nrc.gov/reading-rm/doc-collections) and reports (e.g. *USNRC*, 2001).

These latter publications include Generic Letters (*GL*) and periodic revisions of the "Generic Aging Lessons" (*GALL*) report. Of current interest are recent studies by both the *USNRC* (Muscara, 2007) and the Electric Power Research Institute (*EPRI*, 2008) to assess future modes of material degradation of reactor structural materials, including carbon and low alloy steels. A similar study is now underway in Japan under sponsorship of the Nuclear Industrial Safety Agency (*NISA*).

The consequence of these material failures has been primarily economic, in that the failures have led to forced and extended plant outages (therefore entailing the cost of replacement power) together with the cost of component repair/replacement. Rarely has there been a significant safety issue as quantified, for instance, by an actionable change associated with an increase in Core Damage Frequency (ΔCDF). On the other hand there is no question that there have been violations of the General Design Criteria (i.e. a legal requirement) and these have had a significant impact on the public perception of plant safety in some notable cases (e.g. *BAC* at Davis-Besse, *FAC* at Mihama).

These incidents are discussed in some detail in this report, moving logically from general corrosion modes (including *FAC* and *BAC*) to those that are localized (e.g. crevice, pitting, *MIC*, galvanic) and the various sub-modes of Environmentally-Assisted Cracking (*EAC*)). The localized degradation modes are particularly of concern since they are often hard to detect and mitigate before significant damage has occurred. An extended section is assigned in this report to environmentally-assisted cracking since this mode has presented a long-running concern for carbon and low alloy steels. In each case the phenomenology of the degradation mode is described, preparatory to addressing the system parameters that control the kinetics of degradation, the service experience and the potential mitigation approaches.

Central in these discussions is an assessment of the quantitative understanding of the mechanism of a specific degradation mode, since it is this knowledge that gives the fundamental basis for managing degradation in the future, especially when the reactors may operate under changed operating conditions. These future operating modes of concern involve power uprates, extended licensed life and load following, all of which might be expected to exacerbate materials degradation. For instance, power uprates are associated with increased coolant flow in the primary system, thereby leading to exacerbated flow assisted corrosion and to increased flow-induced vibration. Similarly, load following will involve frequent dynamic loading, which invariably accelerates the various environmentally-assisted cracking submodes. Extending operating licenses from, for instance, 40 years to 60 years, or even 80 years, will impact on degradation modes such as irradiation embrittlement (due to the increased neutron fluence), thermal embrittlement (due to aging phenomena occurring over the extended operating time at temperature), and to fatigue (due to the fact that only a specific number of fatigue cycles are allowable by the regulatory requirements associated with the *ASME* Section III design curve). Moreover, if employed, longer fuel cycles will lead to extended times between inspections, which impact on the effective management of the degradation phenomena.

Before addressing the specific corrosion–based issues, however, some of the physical metallurgical aspects of the carbon and low-alloy steels are addressed, since the details of the material compositions and structure are central to satisfying the mechanical property criteria in the *ASME* Section III code, and they can also have an effect on the kinetics of some of the environmentally-assisted degradation modes.

2 Physical metallurgy of carbon and low-alloy steels

Carbon and low alloy steels are iron-based alloys with small amounts of elemental additions (carbon, chromium, nickel, etc.) that are made for reasons of strength, ductility, formability, grain refinement, weldability, etc., Table 2-1 and Table 2-2. (Note only a sampling of the steels are shown in these tables, since the list is significantly longer when taking into account the different manufacturer decisions and specifications in different countries. The purpose here is to illustrate the ranges in composition). These steels are used in the reactor in a variety of forms including seamless piping, forgings, castings, and plate. The specific carbon or low alloy steel / component combinations that are used in a particular reactor vary between reactor design and manufacturer but, in general:

- In older *PWR*'s and *BWR*'s, reactor pressure vessel vertical sections were manufactured from rolled low alloy steel A533 Gr.B Class 1 plates that were then welded to form a right cylinder. Newer plants use ring forgings of A508 Gr 3. These cylinders are then clad on the internal surface with a 5 to 7 mm layer of Type 308 stainless steel, and then stress relieved during a Post Weld Heat Treatment (*PWHT*) at 595°C-620°C for one hour per 25 mm thickness of steel. The composition of the C-Mn-Mo low alloy steels have more severe limitations on the Cu, S, P and V contents for the high flux beltline region, since these elements increase the extent of irradiation embrittlement.
- The top and bottom heads of the pressure vessel in *BWR*s and *PWR*s are generally clad low alloy steel A508 Gr.2 Class 1 or A508 Gr3 forgings, using the same cladding/heat treatment conditions as for the vertical sections, detailed above. Note that, after fabricating the vertical sections and the top and bottom heads, all three subassemblies are welded together to form the primary pressure vessel and then given a further *PWHT*; thus the total *PWHT* time for any one subcomponent may be up to 40 hours.
- Steam generator shells of *PWR*s are low alloy steel A533 Gr.A Class 1 or Class 2 plates or A508 Gr3 forgings which, like the pressure vessel, are stress relieved. The secondary side of the steam generator is not usually clad.
- Steam generator tube sheets in *PWR*s may be A508 Gr.2 Class 1 or A508 Gr.2 Class 2, or A508 Gr3, with cladding on the primary side in the bottom head.
- Steam generator channel heads in *PWR*s may be A216 Gr.WCC or A508 Gr3.
- The pressurizer shell in *PWR*s may be low alloy steel A516 Gr.70 or A533 Gr.B plate or A508 Gr3 forgings with internal cladding.
- Reactor coolant piping for *PWR* primary circuits may be, in some designs, seamless carbon steel with internal austenitic steel cladding rather than the more commonly used cast or wrought austenitic stainless steels pipes. As will be discussed later, the recirculation piping in *BWR*s is usually stainless steel, although unclad A333 Gr. 6 carbon steel piping is used in the main steam and the feedwater lines. In all plants the piping in the lower temperature emergency core cooling and auxiliary/support systems is usually seamless A105 or A106 Gr.B carbon steel.
- Steam turbine discs and rotors are forged components using the low alloy steels A469, A470 and A471, with the desired mechanical properties being achieved by appropriate heat treatment and alloy composition.

The mechanical properties of these steels (Table 2-3) are directly related to the alloy microstructure and the phases present, and how these are controlled by the composition and processing parameters.

Table 2-1: American Society for Testing Materials (*ASTM*) compositional specifications for ferritic and bainitic carbon and low alloy steels concentrations given in units of wt % (numbers in parentheses refer to the note number at the bottom of the table).

ASME/ASTM or AISI Spec	C max	Mn	P max	S max	Si	Cu max	Ni	Cr	Mo	V max	Typical use
Ferritic steels											
A105	0.035	0.6-1.05	0.035	0.04	0.1-0.35	0.4 (1)	0.4 max (1)	0.3 max (1)	0.12max (1)	0.05	Forging
A106 Grade B	0.3	0.29-1.06	0.035	0.035	0.10 min.	0.4 (2)	0.4 max (2)	0.4 max (2)	0.15 max (2)	0.08 (2)	Seamless Piping
A216 Grade WCB	0.3	1.00max	0.04	0.045	0.6 max	0.3 (3)	0.5 max (3)	0.50 max (3)	0.2 max (3)	0.03 (3)	Casting
A302 Grade B	0.25	1.15-1.50	0.035	0.035	0.15-0.40				0.45-0.6		PV Plates
A333 Grade 6	0.3	0.29-1.06	0.035	0.035	0.1max						Feedwater piping
A508 Grade 3	0.25	1.2-1.5	0.025	0.025	0.15-0.4		0.4-1.0	0.25 max	0.45-0.6	0.05	Forgings
A516 Grade 70	(4)	0.85-1.2	0.035	0.035	0.15-0.4						Plates
A533 Type A	0.25	1.15-1.5	0.035 (5)	0.035 (5)	0.15-0.4	(5)			0.45-0.6	(5)	PV Plates
A533 Type B	0.25	1.15-1.5	0.035 (5)	0.035 (5)	0.15-0.4	(5)	0.40-0.7		0.45-0.6	(5)	PV Plates
Bainitic steels											
1Cr1Mo0.25V	0.33	0.85			0.25			1	1.25	0.25	Feedwater piping
2Cr1Mo (Grade 22)	0.026	0.49	0.012	0.009	0.28	0.05		2.42	0.98		Cross around piping
NiCrMoV (A469 Cl.8)	0.28	0.6	0.015	0.018	0.15-0.3		3.25-4.0	1.25-2.0	0.3-0.6	0.15	Steam turbine
NiCrMoV (A470 Cl.8)	0.35	1.0	0.015	0.018	0.15-0.35		0.75	0.9-1.5	1.0-1.5	0.3	wheels and
NiCrMoV (A471 Cl.8)	0.28	0.7	0.015	0.015	0.15-0.35		2.0-4.0	0.7-2.0	0.2-0.7	0.05	rotors

Notes

1 Sum of Cu,Ni,Cr,and Mo shall be <1.00 wt.%; and sum of Cr and Mo shall not exceed 0.32 wt.%

2 Limits for V and Nb may be increased to 0.1 wt.% and 0.05 wt.% respectively

3 Sum of Cr and Ni shall not exceed 0.32wt.%

4 Carbon max. varies with thickness of plate; 0.5"-2":0.28 wt.%max.; 2"-4": 0.30 wt.% max.; 4"-8": 0.31 wt.%max.

5 For reactor beltline; Cu <0.1 wt.%max., P< 0.012 wt.%max.;S<0.015 wt.%max. and V <0.05 wt.%max.

Table 2-2: Composition of high strength low alloy steels.

ASTM Spec	C	Mn	P max	S max	Si max	Cu max	Ni	Cr	Mo	V max	Typical use
4340	0.38-0.43	0.6-0.8	0.035	0.04	0.15-0.35		1.65-2.0	0.7-0.9	0.2-0.3		Bolting
4140	0.38-0.43	0.75-1.0	0.035	0.04	0.15-0.35			0.8-1.1	0.15-0.25		

Table 2-3: Room temperature mechanical properties of carbon and low alloy steels (Cl 1 and Cl 2 refer to "Class 1" and "Class 2").

Grade	Yield strength Ksi	Tensile strength Ksi	Elongation %
A105	30	70	22
A106 Gr.B	35	60	30 (Long.):16.5 (Trans.)
A216 Gr.WCB	36	70(min.)- 95 (max.)	22
A302 Gr.B	50	80 (min.)- 100 (max.)	18
A508 Gr.2	50 (Cl.1): 65 (Cl.2)	80-105 (Cl.1) : 90-115 (Cl.2)	38 (Cl.1) : 35 (Cl.2)
A508 Gr.3	50	80 (min.)-105 (max.)	18
A516 Gr70	38	70(min)- 90 (max.)	21
A533 Gr A	50 (Cl1):70 (Cl.2)	80-100 (Cl.1) :90-115 (Cl.2)	18 (Cl.1): 16 (Cl 2)
A533 Gr.B	50	80 (min.)-100(max.)	18

2.1 The metallurgical phases; their microstructures and their effect on mechanical properties

The basis for understanding carbon and low alloy steel microstructures and, therefore, their properties is the Fe-C phase equilibrium diagram, Figure 2-1. This diagram is based on thermodynamic equilibrium conditions, and provides guidance as to the phases (e.g. austenite, ferrite, cementite) that might be present in the microstructure when processed under slow cooling conditions. This diagram is based on the relative thermodynamic stabilities of these phases in the different temperature ranges encountered during fabrication (e.g. hot forming, welding), subsequent heat treatment and, sometimes, operation.

Carbon and low alloy steels used for structural components in nuclear plant contain (Table 2-1) less than 0.3 w/o (i.e. bounded by the red line in Figure 2-1), since lack of ductility and toughness with higher carbon contents limit the alloys' usefulness for structural components. Note, however, that when higher strengths are required, as with pressure head or pump bolting where the material is not normally in contact with the coolant, higher carbon contents are specified, (Table 2-3). For brevity, attention here is focused on steels with carbon contents in the range of 0.1-0.3w/o. Since the carbon content in such alloys is less than the "eutectoid" composition (which contains 0.8 w/o carbon) in the binary Fe-C case (Figure 2-1), these alloys are known as hypoeutectoid steels.

Figure 2-1 shows that carbon atoms are in solid solution in such alloys over the temperature range of approximately 800°C to 1430°C. Under these conditions the carbon atoms are located at interstitial positions between the Fe atoms in the face centered cubic (fcc) iron lattice; this phase is called austenite (γ). Upon slow cooling below approximately 800°C the γ phase starts to transform to the body centered cubic (bcc) form of iron, called ferrite (α). The α phase nucleates at, and grows from, the high energy austenite grain boundaries as shown schematically in Figure 2-2(a) and Figure 2-2(b). Further (slow) cooling below a "eutectoid" temperature of 727°C causes the remaining austenite to transform to "pearlite" which is a mixture of ferrite (containing a maximum of 0.022w/o carbon) and cementite (Fe_3C), (denoted as Cm in Figure 2-1). The morphology of pearlite is a lamellar mixture of ferrite and cementite, Figure 2-2(c).

Importantly Figure 2-1 does not show what happens when rapid cooling limits the carbon atom diffusion and results in much harder microstructures such as "martensite" and "bainite". These non-equilibrium microstructures will be discussed momentarily since they play a crucial role in determining the range of mechanical properties that can be obtained, depending on the alloying elements and heat treatments applied.

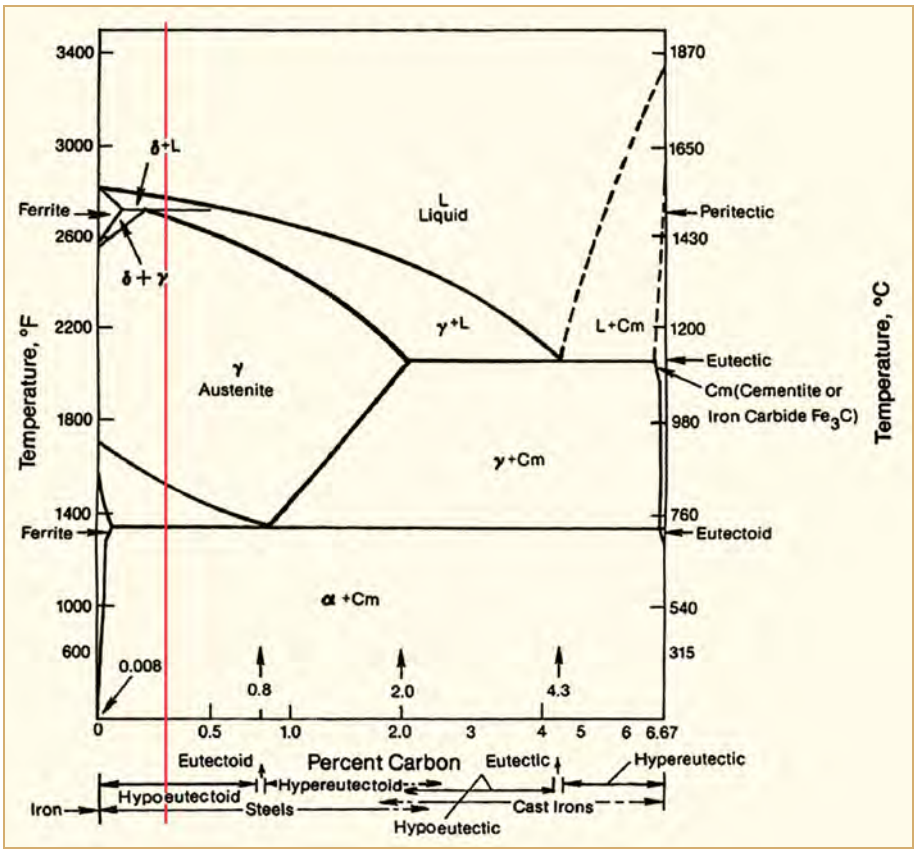

Figure 2-1: Iron-carbon equilibrium phase diagram. Note that the red line denotes the maximum carbon content in structural steels used in water-cooled reactors.

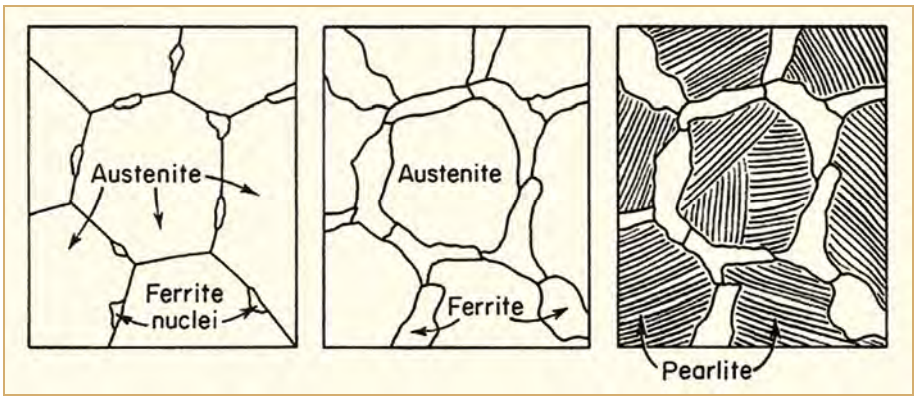

Figure 2-2: Three stages in the formation of ferrite and pearlite during slow cooling of the austenite phase of a hypoeutectoid steel, Reed-Hill, 1964.

In order to understand better the behavior of carbon and low alloy steels, the microstructures and their sensitivity to processing (heat treatment, as well as elevated temperature service) will be discussed below.

Austenite

The face centered cubic austenite phase is, as seen from Figure 2-1, stable at elevated temperatures over a relatively wide carbon content range. However at temperatures below about 800°C it is not stable for the carbon and low alloy steels and operating temperatures relevant to *LWR*s. This is especially the case for steels containing significant amounts chromium and silicon which stabilize the ferrite phase in comparison to the austenite phase. By contrast, alloying additions such as nickel stabilize the austenite phase to lower temperatures and this is the basis of the austenitic stainless steels.

There is continuity between the stability of the ferrite and austenite phases as a function of the iron, chromium and nickel contents, as indicated in Figure 2-3 by the 400°C isotherm of the iron-chromium-nickel equilibrium phase diagram. This behavior serves as a basis for a wide range of important alloys. Of special interest in Figure 2-3 are the compositions of the common alloys used in *LWR*s. Of particular note with respect to the carbon and low alloy steels are; (a) the austenitic stainless steels, such as Type 304, containing chromium and nickel contents (of the order of 18 w/o and 8w/o respectively) where the austenite phase is metastable at room temperature due to the high nickel content, and (b) the ferritic stainless steels, such as Types 410 and 17-4PH,where the ferrite phase is stable due to smaller amounts of nickel and chromium contents of the order of 12-17 w/o.

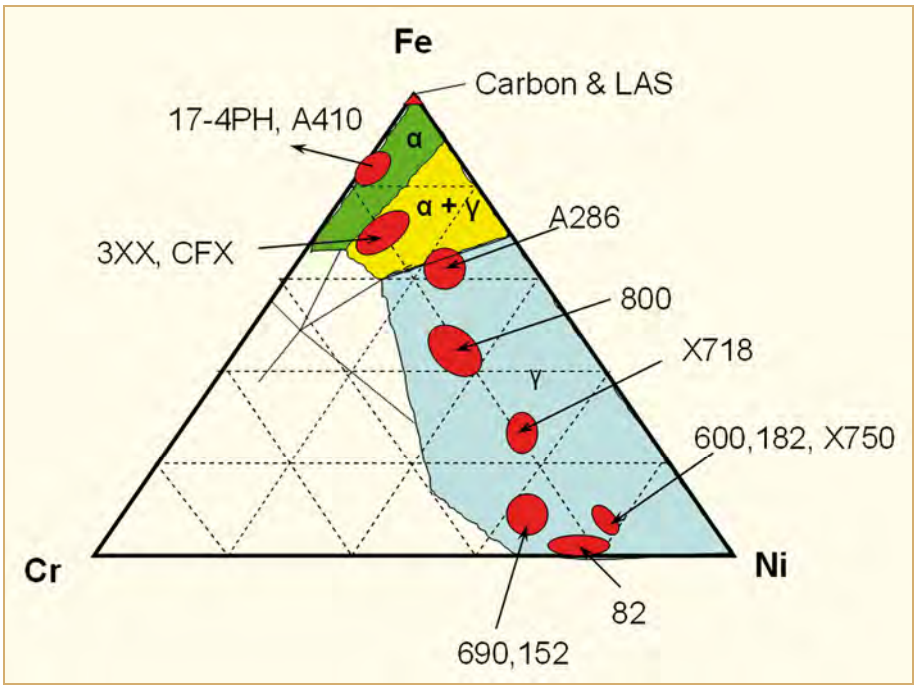

Figure 2-3: Simplified ternary equilibrium diagram for iron, chromium and nickel at 400°C.

Although the austenite phase is not stable at *LWR* operating temperatures in the carbon and low alloy steels in Table 2-1, the presence of "prior austenite" grain boundaries can be a site for segregation of elements such as phosphorous, antinomy, tin and arsenic in quenched and tempered steels. This solute segregation, which typically occurs in the 400-500°C temperature range, is retained at the lower temperatures and can give rise to temper embrittlement and intergranular stress corrosion cracking in some of the steam turbine low alloy steels. These aspects are discussed later.

Ferrite

The ferrite phase is a solid solution of iron and carbon, and one or more alloying elements such as silicon, chromium, manganese and nickel. The smaller elements such as carbon occupy interstitial sites in the body centered cubic ferrite (α) phase and can diffuse relatively rapidly compared with other larger alloying element atoms. As will be discussed later, this diffusion aspect has an impact on the formation kinetics and morphologies during phase transformations. The solubility of carbon in the ferrite phase is low; for example it has a maximum solubility of 0.022w/o at the eutectoid temperature, 727°C, and decreases to below 0.005w/o at room temperature in a binary Fe-C alloy. However, in spite of this low solubility, carbon (and nitrogen and phosphorus) can have a marked effect on the yield stress of the ferrite phase, Figure 2-4.

A further factor that leads to an increase in the yield stress is a decrease in the ferrite grain size, as shown in Figure 2-5. This dependency is described by the Hall-Petch relationship (Equation 2-1) and, as will be seen later, this type of relationship between yield stress and the size of a dominant physical feature is observed in other phases and phase mixtures.

Equation 2-1: $$\sigma_y = \sigma_\circ + k_y d^{-0.5}$$

where σ_y is the yield stress, $\sigma_\circ$ and k_y are constants, and d is the ferrite grain size.

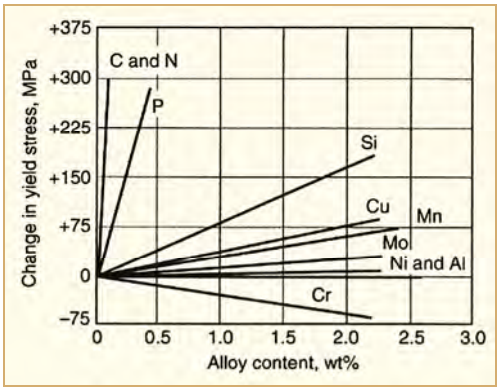

Figure 2-4: Influence of solid solution elements on the changes in yield strength of low-carbon ferritic steels, Pickering, 1978

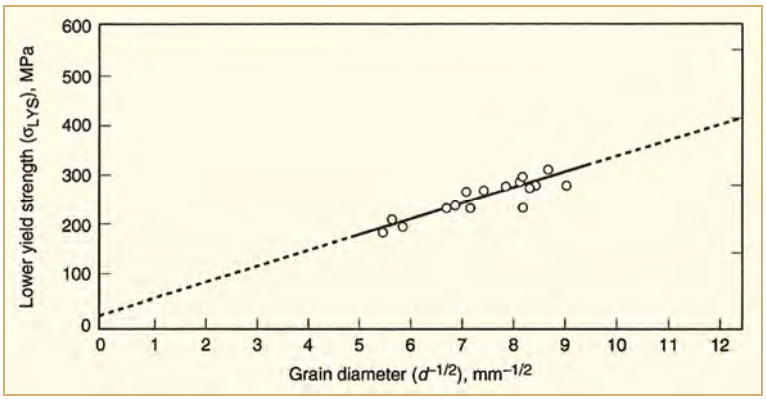

Figure 2-5: Hall-Petch relationship in low-carbon ferritic steels, Microalloying, 1977.

The thermomechanical and alloying methods for refining the grain size, and thereby controlling the mechanical properties, will be described later.

Pearlite

As indicated in Figure 2-1, and schematically in Figure 2-2, the ferrite phase nucleates and begins to grow at the austenite grain boundaries during slow cooling of a hypoeutectoid steel below approximately 800°C. During this process the ferrite rejects carbon, and the carbon content in the remaining austenite phase increases until, under equilibrium conditions, it reaches 0.8w/o at the eutectoid temperature, 727°C in a Fe-C alloy. Below that temperature the remaining austenite transforms (Figure 2-6) to a lamellar mixture of nearly pure Fe (the ferrite phase) and carbon-rich Fe_3C (cementite); this mixture of phases is known as pearlite. Thus, a typical slowly cooled steel with low to medium carbon content (for example <0.5w/o C) will have a structure that is a mixture of ferrite that formed above the eutectoid temperature and pearlite. Increasing carbon content increases the fraction of pearlite.

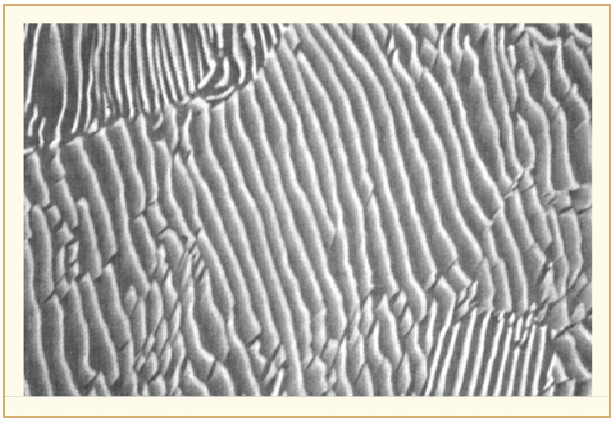

Figure 2-6: Scanning Electron Microscope (*SEM*) micrograph of pearlite showing cementite and ferrite lamellae (10000X), Vander Voort & Roosz, 1984.

These transformations involve nucleation and growth phenomena, which depend on temperature/time controlled diffusion processes for the carbon, manganese, nickel, chromium and molybdenum alloying elements. The effect of these conditions may be illustrated on Time-Temperature-Transformation (*TTT*) diagrams, which relate to the extent of the transformation occurring during an iso-temperature anneal for a given time (e.g. a post weld heat treatment), or on Continuous-Cooling-Transformation (*CCT*) diagrams which relate to the transformations that occur during a cooling process following a normalization or homogenizing heat treatment in the austenite phase stability region. There are differences in the kinetic details in such *TTT* and *CCT* diagrams, but, for brevity, these will not be discussed and emphasis is placed on the essential common features.

The *TTT* diagram for a eutectoid steel (containing 0.8 w/o carbon) is discussed initially, before moving to more relevant lower carbon steel compositions for nuclear plant structures. The physical process for the formation of a pearlite colony in the austenite phase involves the nucleation of a Fe_3C platelet at an austenite grain boundary. This nucleation will be accompanied by carbon depletion adjacent to the platelet, which then triggers the nucleation and growth of an associated ferrite platelet. The subsequent growth of the Fe_3C and ferrite lamellae in the pearlite colony will depend on the diffusion kinetics of carbon in the austenite phase, Figure 2-7. The rates of nucleation and growth of the pearlite colonies as a function of temperature are different (Figure 2-8) leading to the conclusion that nucleation is the rate limiting process at temperatures just below the eutectoid temperature (727°C), and the growth of the pearlite colony becomes rate limiting at temperatures below 655°C, Thus, as indicated in the *TTT* diagram for this eutectoid steel (Figure 2-9), the extent of transformation from austenite to a (mixed ferrite plus Fe_3C) pearlite colony exhibits a characteristic temperature–time dependency with the maximum rates of austenite transformation occurring around 550°C.

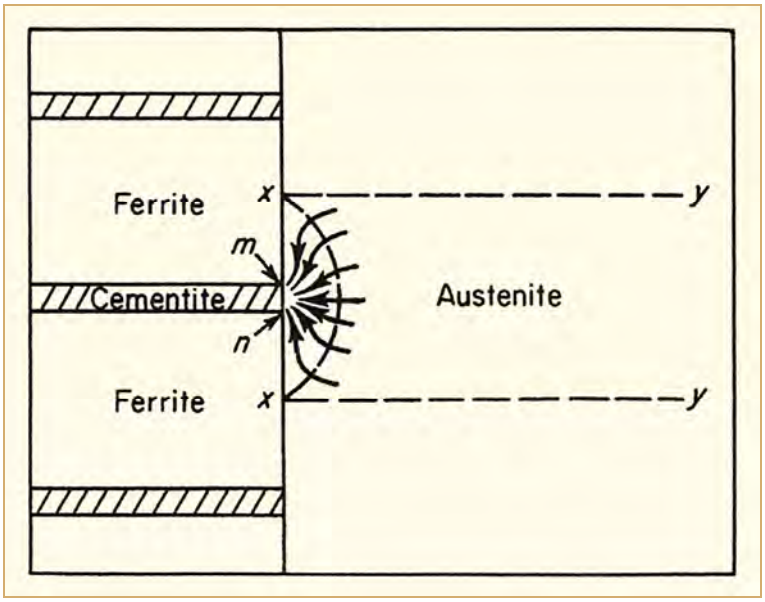

Figure 2-7: Flow of carbon atoms into a cementite plate during growth of pearlite, Reed-Hill, 1964.

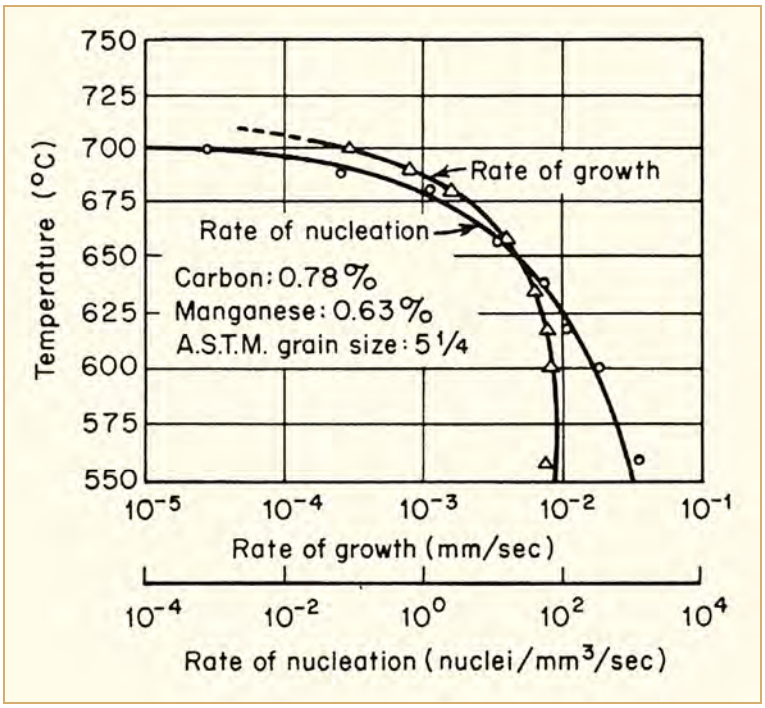

Figure 2-8: Variation of the pearlite nucleation and growth rates for a eutectoid steel, Mehl & Dube, 1951.

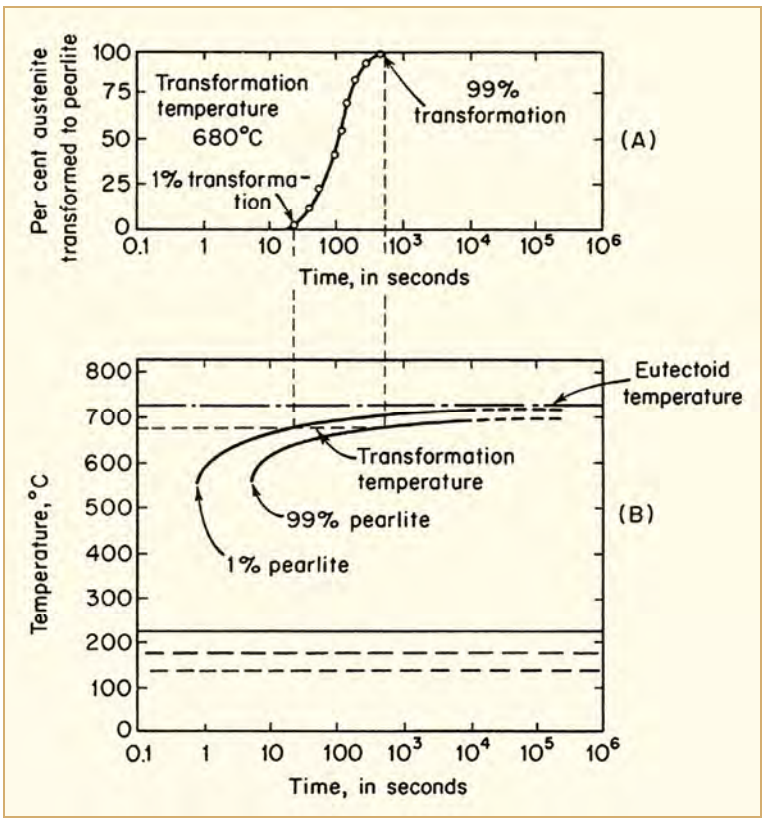

Figure 2-9: *TTT* curves for the percent transformation in a eutectoid steel of austenite to pearlite, Reed-Hill, 1964.

The pearlite structure represents a composite made up of a soft ductile ferrite phase and the harder carbide compound, Fe_3C. As might be expected the mechanical properties of the pearlite mixture reflect this composite character (Hyzak & Bernstein, 1976) with the yield stress (σ_y) being a function (Equation 2-2) of the inter-lamellar dimensions (λ) the pearlite colony size(d_c) and the prior austenite grain size (d_γ):

Equation 2-2: $$\sigma_y = 52.3 + 2.18(\lambda)^{-0.5} - 0.4dc^{-0.5} - 2.88d_\gamma^{-5}$$

where the yield strength is in units of MPa and the structure dimensions are in units of mm.

The inter-lamellar spacing decreases as the transformation temperature decreases, thereby giving a practical approach for achieving high yield strengths and good wear resistance (e.g. strengths of the order of 800 MPa are possible for inter-lamellar spacing of the order of 90 nm). However, such fully pearlitic, eutectoid steels have limited ductility and exhibit poor fracture resistance and are not used in *LWR* structural components. Consequently, lower carbon steels with lower pearlite contents are usually preferred for structural components. For instance 100% of a 0.8wt.% carbon steel microstructure is taken up with pearlite, whereas lowering the carbon content to 0.3wt.% or 0.2wt.% lowers the amount of pearlite in the microstructure to 37% and 25% respectively. This effect on the microstructure is illustrated in Figure 2-10.

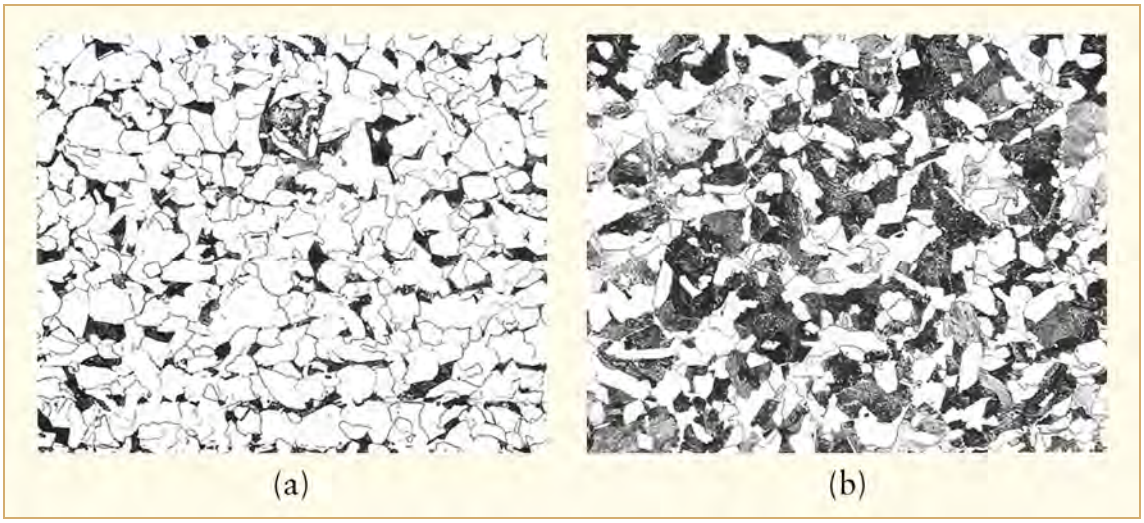

Figure 2-10: Microstructure of typical ferrite-pearlite structural steels at two different carbon contents (Pearlite is the darker component; ferrite is the lighter component) (a) 0.10w/o C and (b) 0.25w/o C. Magnification X200.

As would be expected the mechanical properties of these ferritic-pearlitic steels exhibit a continuous variation with changing carbon content (Figure 2-11), and in particular, a marked improvement in fracture resistance (as quantified by the brittle to ductile Transition Temperature (*TT*) and upper shelf energy measured in a Charpy V-notch test) is observed with decreasing carbon content, Figure 2-12.

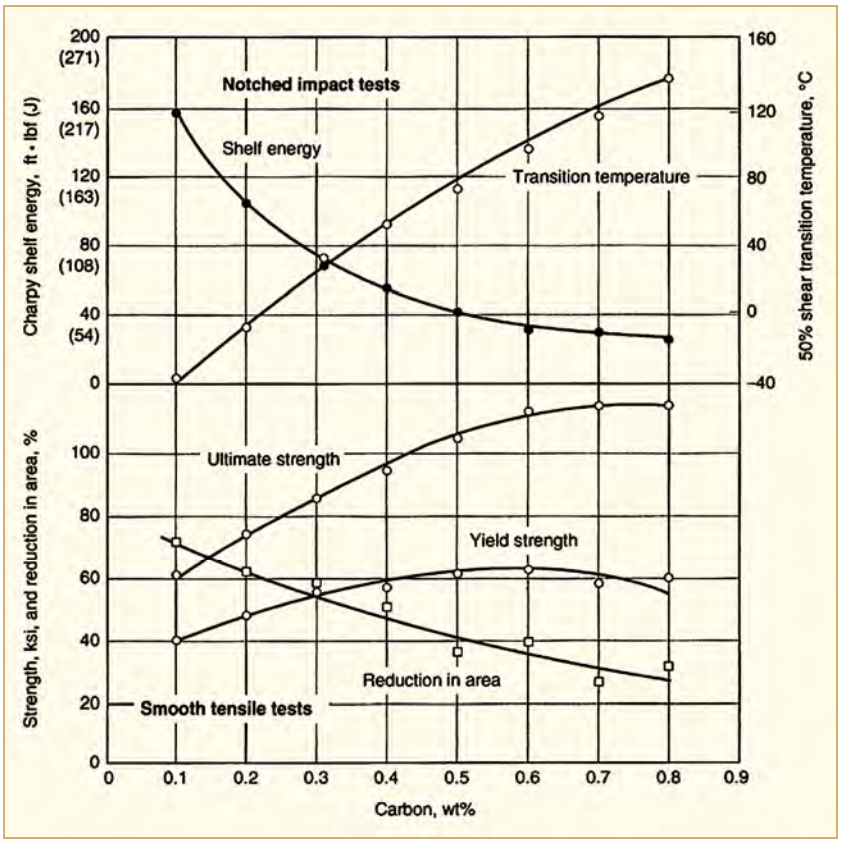

Figure 2-11: Room temperature mechanical properties of ferrite—pearlite steels as a function of carbon content, Krauss, 1980.

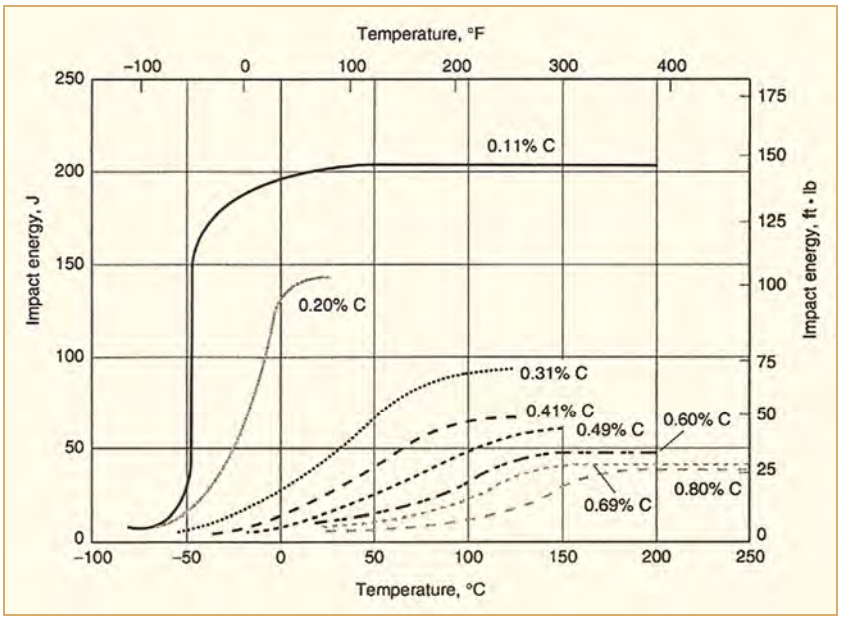

Figure 2-12: Effect of carbon content in ferrite-pearlitic steels on charpy V-notch transition temperature and shelf energy, Roe & Bramfitt, 1990.

Thus a reasonable compromise between strength, ductility and fracture resistance can be achieved for a slowly cooled ferritic-pearlitic steel containing 0.25w/o carbon. As seen in Equation 2-3. and Equation 2-4, modifications to the yield stress and the *TT* for such a carbon steel can be obtained (Pickering, 1978 via refinement of the ferrite grain size, and making manganese or silicon alloying additions; note, however, that although some strength increases may be obtained via phosphorus and free nitrogen (N_f) additions, such modifications are avoided due to potential deleterious effects on toughness (see Equation 2-4).

Equation 2-3: $\sigma_y = 53.9 + 32.34\ (Mn) + 83.2\ (Si) + 354.2(N_f) + 17.4\ d^{-.5}$

Equation 2-4: $TT = -19 + 44(Si) + 700\ (N_f)^{0.5} + 2.2(P) - 11.5d^{-0.5}$

As a result, ferrite grain refinement is obviously a desirable fabrication goal, and this may be achieved either by controlled metal working and/or by microalloying. In the former case the component is warm fabricated at temperatures below the austenite recrystallization temperature, such that a "pancake" austenite grain shape is obtained; during subsequent nucleation of the ferrite phase at austenite grain boundaries the final size of the ferrite grain growth is restricted by the flattened austenite grain shape. In the latter case, small alloying additions of vanadium, niobium or titanium form small carbides or carbonitrides which retard grain growth and promote a fine grain structure in the ferrite.

The previous discussion emphasized the time-temperature dependence of the transformation from the high temperature austenite structure to the low temperature equilibrium structure of ferrite plus pearlite in slowly cooled steels. The obvious question arises; "What happens if the steel is cooled so rapidly that the ferrite plus pearlite cannot form?" This is the case where the steel is quenched from high temperatures at a rate to miss the nose at 550°C in the *TTT* curve in Figure 2-9 for an eutectoid steel and in Figure 2-13 for an hypoeutectoid steel. In such a case two possibilities exist. The structure may transform to either bainite and/or martensite. These transformations are now discussed.

Bainite

Unlike the pearlite microstructure, which is lamellar (Figure 2-6), the bainite microstructure is mainly acicular (Figure 2-14) with the details of the carbide/ferrite morphology being dependent on the transformation temperature range. At the higher transformation temperatures circa 400°-600°C, the fine carbide particles deposit in the ferrite lath boundaries, whereas at the lower transformation temperatures the carbides deposit within the ferrite laths. Initially this difference between the two bainite microstructures led to the nomenclature of "upper bainite" and" lower bainite" (referring to the transformation temperature range), but this has been superceded by a wider classification based on the detailed microstructure. Regardless of the details of this classification system, the practical importance of this bainitic microstructure is that it exhibits high yield strength (ranging from 450 to 950 MPa) with good fracture resistance, unlike the ferritic/pearlitic microstructure.

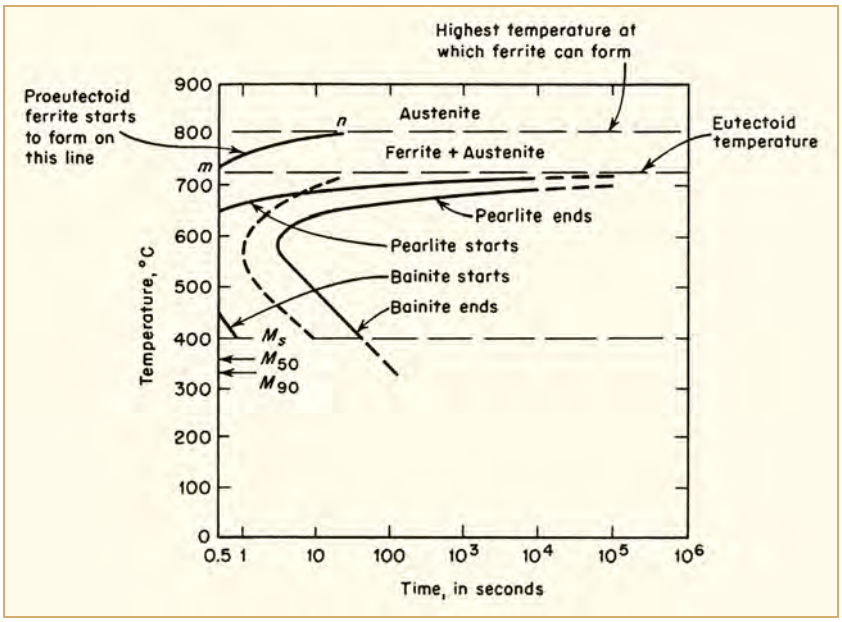

Figure 2-13: Isothermal transformation diagram for a 0.35w/o C, 0.37w/o Mn hypoeutectoid steel, United States Steel Corporation, 1951.

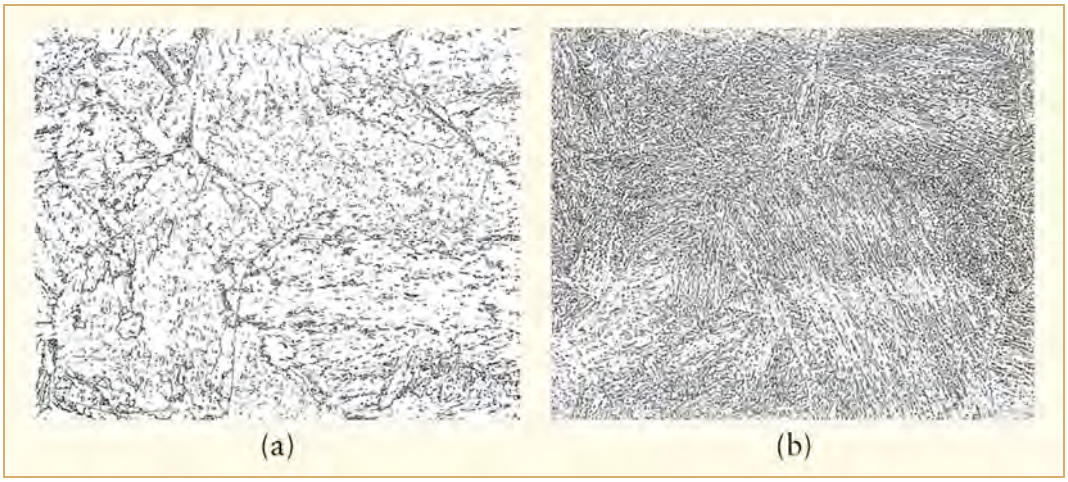

Figure 2-14: Bainite microstructure (a) "Upper Bainite" (b) "Lower Bainite" X500.

As with the ferritic and pearlitic steels the strength of the bainitic steels depends markedly on the dimensions of the microstructural features, with the higher strength values being associated with the lower transformation temperatures where the microstructural dimensions are finer; for instance, in Equation 2-5, the yield stress is a function of the bainite lath size (d) and the number of carbides (n) in the plane of the section, Honeycombe & Pickering, 1972:

Equation 2-5: $$\sigma_y = -194 + 17.4d^{-0.5} + 15\,n^{0.25}$$

where the yield stress is in units of MPa.

The effect of alloying additions (such as nickel, chromium, manganese and, especially, molybdenum) in delaying the transformation kinetics of the austenite to (ferrite and pearlite), and thereby enhancing the formation of bainite over a wide cooling rate range is illustrated in Figure 2-15. It is seen that for the 4340 low alloy steel (containing 0.78w/o Mn, 1.79w/o Ni, 0.8w/o Cr and 0.33w/o Mo) cooling the component at 0.33°C/sec. will allow the formation of bainite (that has satisfactory mechanical properties) over a wide cooling rate range (and, hence, component thicknesses) and will avoid the transformation of the austenite to ferrite and pearlite[6] (which have less desirable mechanical properties). This is particularly important in thick section components, such as turbine rotors and discs where a uniform microstructure is required.(see compositions of the bainitic steels in Table 2-1.

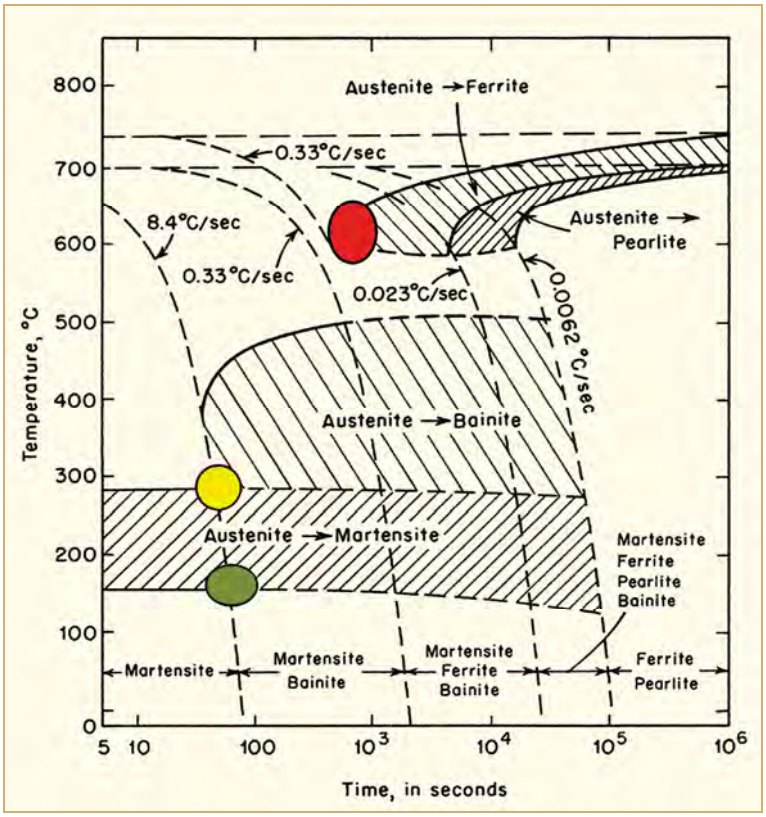

Figure 2-15: Continuous cooling diagram for 4340 steel, United States Steel Corporation, 1948. The colored circles refer to transformations that are discussed in the text.

[6] Shown as the red circle in Figure 2-15

Although the bainitic structure generally provides a good balance between strength and toughness, it can suffer from temper embrittlement when slowly cooled or isothermally heat treated in the temperature range 400° – 500°C. This phenomenon is associated with the presence of P, As, Sn or Sb in the prior austenite grain boundaries (King & Wigmore, 1976) and can give rise to a reduction in fracture toughness and an increase in stress corrosion cracking susceptibility in caustic environments in a specific corrosion potential range. Temper embrittlement can be reversd (McMahon, 1976 and Roberts, 1981), however, by annealing the bainitic structure at temperatures in excess of 600°C (followed by rapid cooling) and, since higher purity castings do not exhibit temper embrittlement, by putting compositional limits on the damaging tramp elements (e.g.<0.005wt.%P, <0.01wt.%Sn) and control of other alloying elements such as Si, Mn, Cr which can promote the impurity segregation to the prior austenite grain boundaries. The addition od ~1w/o Mo also limits temper embrittlement. Alternatively improved casting practice may be used such as ElectroSlag Remelting (*ESR*), Electroslag Hot Topping (*ESHT*) or Central Zone Remelting (*CZR*).

Martensite

All of the transformations so far discussed depend on nucleation and growth processes. Hence, the kinetics of the formation of ferrite, pearlite and bainite will depend on the combinations of temperature and time associated with iso-thermal annealing or the rates of cooling following, for instance, heat treatment or welding. However rapid cooling or quenching can suppress the formation of these structures and give rise to a non-equilibrium, supersaturated solution of carbon in iron. The result is a distorted lattice structure and the formation of "martensite" from the austenite via a diffusionless phase transformation to form a body centered tetragonal (bct) phase. This microstructure can extend over the whole engineering component, assuming that the required cooling rate can be achieved at the various depths below the quenched surface. For instance in Figure 2-15 it is seen that, if the structure is cooled from temperatures in excess of 700°C at rates faster than 8.4°C/sec., the formation of bainite from the austenite phase does not start and, instead, martensite forms once the temperature of the structure reaches a "Martensite start" (M_s)[7] temperature; transformation is complete once the temperature reaches a "Martensite finish" (M_f)[8] temperature.

The values of M_s and M_f depend on the alloy content (Andrews, 1965) and both critical temperatures will decrease, for instance, with increasing carbon content (Figure 2-16) as well as additions of manganese, chromium, nickel and molybdenum, Equation 2-6:

[7] Shown be the yellow circle inFigure 2-15
[8] Shown by the green circle in Figure 2-15

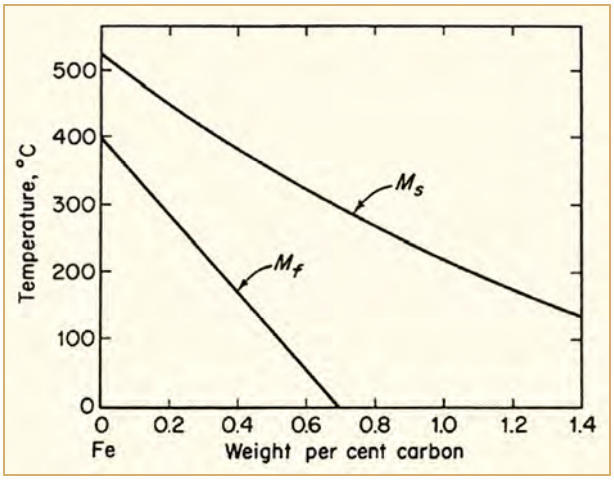

Figure 2-16: Variation of M_s and M_f with carbon content in steel, Troiano & Greninger, 1946.

Equation 2-6: $M_s = 539 - 423\ C - 30.4\ Mn - 12.1\ Cr - 17.7\ Ni - 7.5\ Mo$

The microstructure of the martensite is acicular being classified as either "lath" or "plate martensite". The former dominates at the lower carbon contents common to the structural carbon steels in *LWR*s.

The fully martensitic steels exhibit high hardness and yield stress, with the yield stress (and hardness) increasing (Figure 2-17) with increasing carbon content and decreasing lath size, Figure 2-18. However, because of their low fracture resistance, these steels are rarely used in the as-quenched fully martensitic state in *LWR* structures.

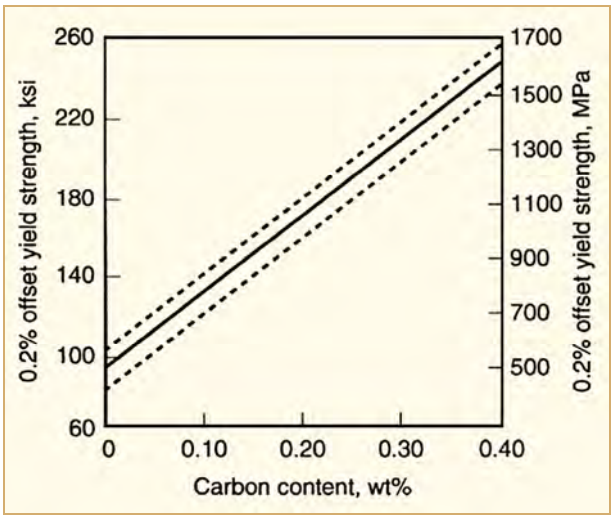

Figure 2-17: Relationship between carbon content and the yield strength of martensite, Leslie, 1981.

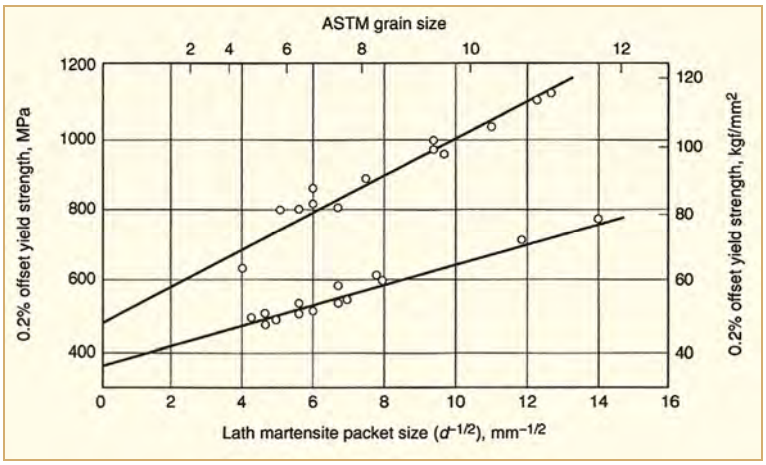

Figure 2-18: Relationship between lath martensite packet size (d) and yield stress of martensite in a 0.2w/o Carbon (upper line) and a Fe-Mn (lower line) steel, Krauss, 1980.

Tempered martensite

A wide range of mechanical properties can be obtained, however, by tempering the martensitic steels, Figure 2-19. This process entails heating the martensite (and retained austenite if the martensitic transformation was not complete) to a temperature below 650°C in order to transform the supersaturated martensite (and retained austenite) to a mixture of ferrite and carbide phases called "tempered martensite". The tempered martensite structure is thus a result of a "quench and temper" heat treatment and is probably the most common form in which higher strength carbon and low alloy steels are used.

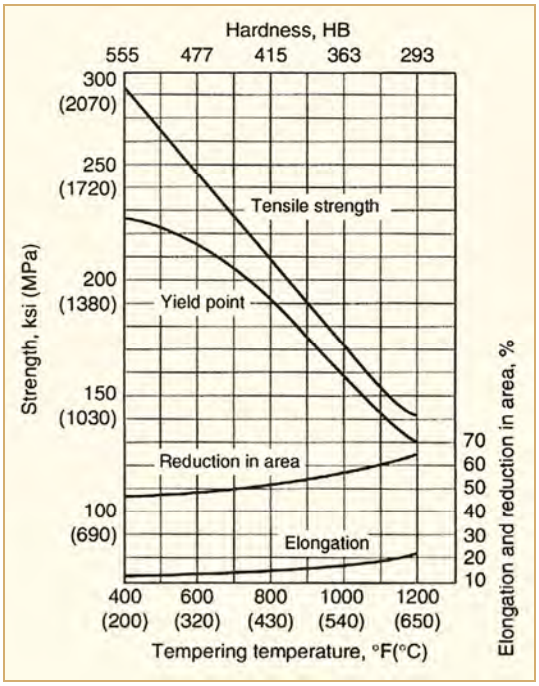

Figure 2-19: Effect of tempering temperature on the mechanical properties of a quenched and tempered (for 1 hour) type 4340 steel, Krauss, 1980.

In summary, it is apparent that a wide range of microstructures can be obtained in carbon and low alloy steels depending on the alloying content and heat treatment. These microstructures can lead to a wide range of mechanical properties depending on the metal temperature and time combinations during isothermal heat treatment (e.g. tempering, *PWHT*) or during cooling from higher homogenizing temperatures or welding.

So far the discussion of the metallurgical phases and microstructure has concentrated on the mechanical properties relevant to the need for satisfactory structural integrity performance in the absence of environmentally-assisted degradation. As will be discussed in some detail in the following sections the mechanical properties and/or the carbon and low alloy steel microstructures can also have an effect on the environmentally-assisted degradation rates. Examples of such interactions include;

- The role of MnS precipitates (associated with sulphur impurities in the steel) acting as sites for pitting, which may then lead to stress corrosion crack initiation, with the subsequent crack propagation rate being dependent on the size, spacing and morphology of the sulphide particles.
- The effect of chromium alloying additions in decreasing the susceptibility of carbon and low alloy steels to flow-accelerated corrosion.
- The segregation of metalloid impurities, primarily phosphorus, to prior austenite grain boundaries leading to temper embrittlement and enhanced intergranular stress corrosion cracking susceptibility of steam turbine disc steels in caustic environments under specific potential conditions.
- The increase in stress corrosion susceptibility due to material properties that change the deformation behavior at a crack tip. Such material properties include increases in yield stress due to coldworking or the onset of discontinuous yielding associated with dynamic strain aging. As will be discussed, there is an expected (Figure 2-20) increase in the stress corrosion crack propagation rate with a decrease in fracture resistance (due to, for instance, cold work, temper embrittlement and irradiation embrittlement).

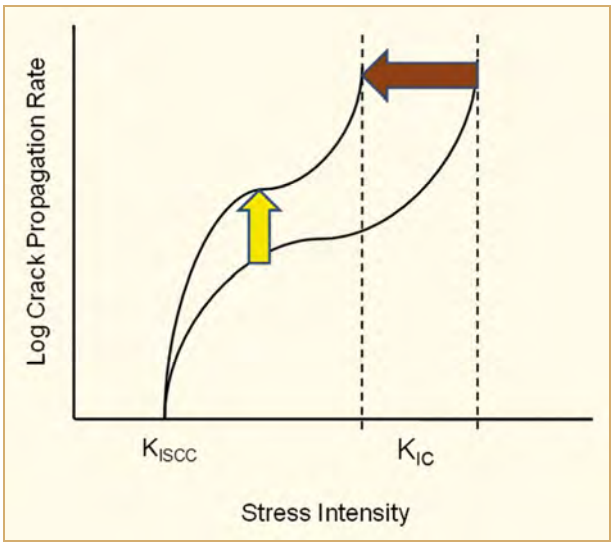

Figure 2-20: Schematic crack propagation rate vs stress intensity curves, illustrating potential effects of decreasing K_{IC} values on crack propagation rate.

3 Uniform corrosion

"Uniform" degradation modes include general corrosion, boric acid corrosion and flow-accelerated corrosion. Such modes result in loss of material over reasonably large areas, defined broadly as greater than 1-2 cm^2, as opposed to localized corrosion that may occur over areas governed by metallurgical inhomogeneity or microstructure.

3.1 General corrosion

General corrosion of all the structural alloys (e.g. austenitic alloys as well as carbon and low alloy steels) is characterized by uniform surface loss through material oxidation, and may be deleterious to plant operation because of:

- The decrease in functionality of a component due to a loss in section thickness.
- The presence of corrosion products that may decrease the heat transfer efficiency upon depositing on e.g. steam generator tubes or fuel cladding.
- The presence of corrosion products which deposit on the fuel cladding surface, become activated and, upon release, increase the radioactivity levels in the Reactor Coolant System (*RCS*) and, in the case of direct cycle *BWR*s, the balance of plant. This sequence of events is discussed in detail in the *LWR* Coolant Chemistry (*LCC2*) Special Topic Report on *CRUD*, (Riess & Lundgren, 2006), primarily for the austenitic alloys (since they present the largest surface volume over which coolant passes before entering the core region).

This subsection of the report concentrates only on the general corrosion phenomena for carbon and low alloy steels. Although the surfaces of the pressure vessel are mostly clad with stainless steel, there are considerable areas of carbon and low alloy steels in the *RCS* of *BWR*s that are not clad, such as the top head of some *BWR*s, the feedwater inlet nozzle, repair regions on the pressure vessel (mainly penetrations), and various piping for feedwater, main steam, etc. Similarly, these steels are not clad with austenitic alloys in secondary systems such as the Emergency Core Cooling System (*ECCS*) of *BWR*s and the secondary water/steam circuits of *PWR*s including the steam generator shell. They are also not clad in tertiary systems for e.g service water, etc. of all types of reactor.

General corrosion issues for carbon and low alloy steels, and the formulation of mitigation actions, are founded on a large body of research over many decades. Thus there is good reason for the judgment that general corrosion of these steels throughout the primary, secondary and tertiary reactor systems is a manageable issue. The following discussion is included, however, since the electrochemical details of general corrosion and the formulation of water chemistry specifications in water cooled reactors forms a basis for understanding other corrosion-based degradation modes.

As explained previously (Ford, 2006) general corrosion rates may be managed by; (a) consideration of the thermodynamically stable (or metastable) species such as dissolved metal cations, oxides, salts, etc. at the metal / water interface and, (b) control of the relevant oxidation and reduction kinetics.

In the case of carbon and low alloy steels in neutral, deoxygenated water circa 200°C the primary reduction process is of hydrogen cations or water, whose equilibrium potential/pH characteristics are shown by the dashed line (a) in Figure 3-1. The counteracting oxidation reaction[9] is the formation of magnetite, Equation 3-1:

Equation 3-1: $3Fe + 4H_2O \rightarrow Fe_3O_4 + 8H^+ + 8e^-$

[9] Note this is a simplified version of the overall reaction since, in actuality, other intermediate species may exist.

4 Localized corrosion

This section addresses materials degradation modes where the corrosion damage occurs over relatively small areas but, potentially, may occur at high penetration rates. The result in such cases may be localized leakage or a decrease in structural integrity. Such degradation modes include crevice, pitting, galvanic and microbiologically-induced corrosion, and environmentally-assisted cracking.

This latter category covers stress corrosion cracking, strain-induced corrosion cracking and corrosion fatigue, and is covered separately in Section 5. These particular degradation submodes receive the most attention in the following discussions since arguably (Muscara, 2007 and *EPRI*, 2008) they present the greatest challenge to maintaining component integrity and developing qualified life prediction and extension capabilities.

4.1 Crevice corrosion

As the title suggests, this phenomenon is associated with crevices inside which a stagnant solution is present, and where there is a mechanism to make that solution more aggressive (e.g. increased acidity or alkalinity, with increased impurity concentration). The crevices may be inherent to the component design (such as at gaskets, lap joints, bolt heads and threads), or may be due to corrosion deposits and sludge piles. The critical factors in controlling this form of attack are; (a) the geometry of the crevice and the conditions that affect the thermalhydraulics, and thereby solution renewal within it and, (b) the mechanisms that change the cationic and anionic concentrations within the crevice.

As indicated schematically in Figure 4-1 there is the possibility that, in environments containing dissolved oxygen, such as in the *BWR RCS* operating under "normal water chemistry" conditions, the site for oxygen reduction is primarily on the exposed surface at the mouth of the crevice, with very little occurring at the crevice tip. A reason for this latter situation is that the convection-controlled transport rate of dissolved oxygen into the crevice cannot balance the removal of dissolved oxygen due to general corrosion on the crevice sides. The resultant separation of the oxygen reduction site at the crevice mouth from the metal oxidation site at the tip of the crevice imposes a potential gradient down the crack, thereby giving rise to potential-driven diffusion of anionic impurities (e.g. chloride) to the crevice tip. In order to maintain electroneutrality it is necessary that there be an increase in acidity within the crevice by hydrolysis of dissolved metal cations, i.e.

Equation 4-1: $$M_{aq}^{z+} + H_2O \rightarrow MO + 2H^+$$

Thus, the environmental conditions of low pH and high anionic impurity concentration are created within the crevice, and this can lead to an increase in metal corrosion rate as discussed previously. The thermal-hydraulics and mechanisms of this mode of crevice corrosion have been extensively researched (Brown, 1974 and *ASTM*, 1972) over the last 30 years and, as a result, control techniques are available.

Classic examples of such environmental changes leading to localized corrosion in *BWR RCS* components are usually associated with stainless steels and nickel base alloys, and occur in the crevices at safe-ends, access hole covers, shroud head bolts and *IRM/SRM* dry tube assemblies, Gordon & Ramp, 1989, Brown & Gordon, 1987. In these cases the potential drop in the crevice is of the order of 700-800 mV and this would give an increase in anionic concentration of the order x 10-100 and a pH decrease of approximately 1-2 units, Ford et al., 1987. Such changes in crevice chemistry are not enough to cause excessive localized corrosion of austenitic stainless steel or Alloy 600 components, but they are sufficient to promote intergranular stress corrosion cracking of these alloys at the tip of the crevice. The obvious remedy for resolving this precursor event to cracking is to improve the water purity and/or remove the potential gradient that is required for the creation of the crevice chemistry by using "hydrogen water chemistry".

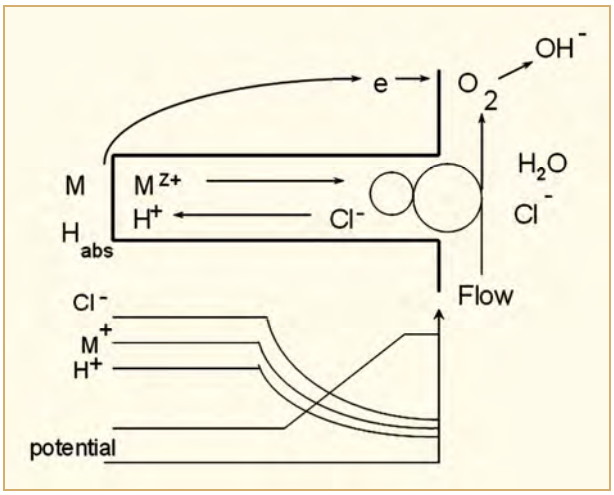

Figure 4-1: Schematic of crevice in aerated solution, indicating the separation of the metal oxidation and oxygen reduction sites, and the consequent changes in pH and anionic concentrations.

It follows that crevice corrosion by this potential difference driven mechanism is not expected in *PWR RCS* systems nor in *BWR RCS* systems operating under *HWC* conditions.

However examples of this potential-driven mechanism of crevice chemistry formation are found in service water systems where the liquid may be naturally aerated (Beavers et al., 1980, Syrett and Coit 1982) and may contain substantial amounts of chloride. A significant number of these examples refer to crevice corrosion of condenser tubes in seawater service. In most cases the problem has arisen due to bad geometrical design. In those cases where this cannot be changed, remedies rely on retubing with stainless steels that contain increased amounts of chromium, nickel and molybdenum. As would be expected, such alloys have a more protective surface oxide that can resist the acidic, chlorinated environment at the crevice tip. The ultimate crevice corrosion resistance is achieved by retubing with titanium alloys, Beavers et al., 1980.

An alternative mechanism for creating a localized aggressive environment occurs on heat transfer surfaces, where concentrations of species change due to their partition between the aqueous and gaseous (e.g. steam) phases, or the evaporation of volatile species. This concentration of acidity, alkalinity or other aggressive non-OH^- anions is called 'hideout' and is observed under specific superheated geometrical conditions that inhibit solution redistribution. A classical example of this is the localized corrosion of carbon steel tube support plates in *PWR* steam generators, as illustrated in Figure 4-2 and, because of the increase in volume of the corrosion product compared to the parent carbon steel plate, this has led to plastic deformation ("denting") of the Alloy 600 tube and subsequent stress corrosion cracking on both the primary and secondary sides of the tube.

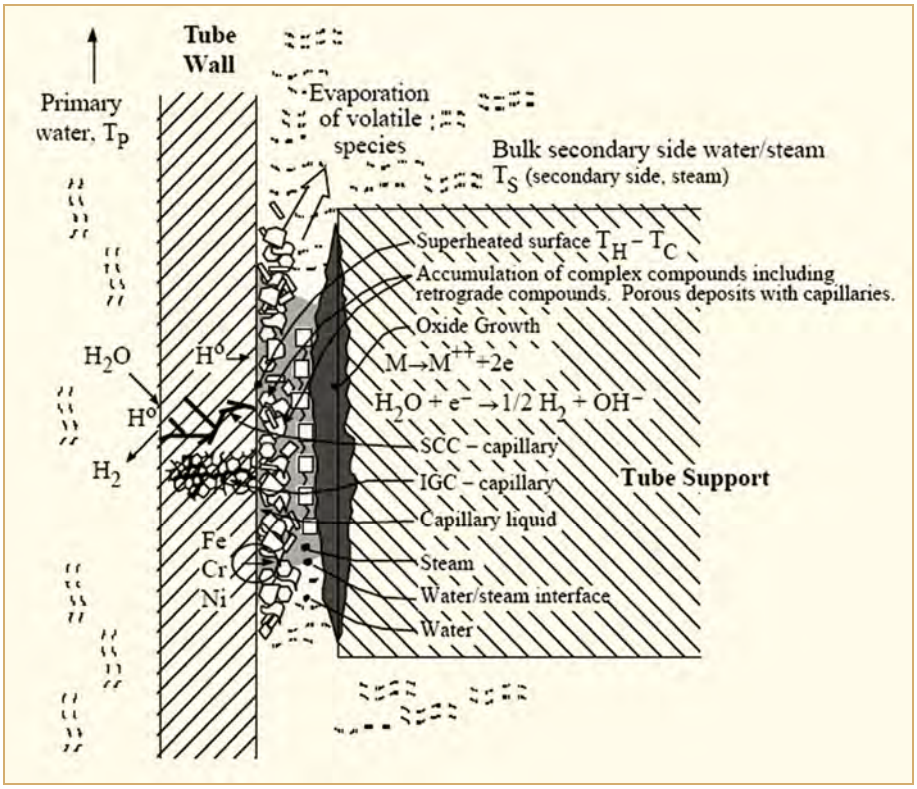

Figure 4-2: Schematic of crevice formed at *PWR* steam generator tube/ carbon steel tube- support, together with the phenomena that give rise to the localized corrosion, Staehle, 2001.

The mechanisms for the creation of such concentrations of impurity species are well recognized, having their origin in corrosion of heat transfer surfaces in fossil-fired plant. The liquid adjacent to the heat transfer surface must have a boiling point equal to the temperature of that surface, but the vapor pressure above that liquid must be equivalent to that of the secondary side pressure. The temperature difference between the primary and secondary sides of a (recirculating) steam generator tube will vary from 45°C at the hot leg and 22°C near the top of the U-bends. Considerable solute concentrations are required in order to accommodate these amounts of superheat and to maintain a liquid phase on the outside of the tube at the secondary side pressure. Different solutes can support different amounts of superheat, You et al., 2002, Scott, 2001, Baum, 2001. For instance (Scott & Combrade, 2006), NaOH will support >25°C superheat, whereas sodium chloride will support <25°C superheat before the solubility limit is reached and precipitation occurs. Thus, as the extent of superheat changes along the tube between the entrance and exit of the *RSG*, the composition of the precipitates trapped in the tube support plate crevice, and the pH of the slurry in that region will change significantly. The changes in composition can be remarkable (Figure 4-3); for instance chloride concentrations of the order of 4000 ppm are possible (Layman et al., 1979) in the tube support plate crevice, in comparison to concentrations of <0.03 ppm in the bulk secondary environment, see Table 3-2.

5 Environmentally-assisted cracking

As mentioned in Section 1, *EAC* is a term used to describe various submodes of cracking, including stress corrosion cracking, strain-induced corrosion cracking and corrosion fatigue. These classifications are guided primarily by the different stress or strain conditions that drive the cracking process and their relationship to various reactor operating modes, Table 5-1. For instance:

- *SCC* is associated with constant stress or strain due to pressure or displacement loading (e.g. bolts, residual stress) under transient free, steady-state power operation.
- Strain induced corrosion cracking (*SICC*) is associated with slow monotonically rising (or very slow cycle) loading that is relevant to reactor start up/ shut down or with thermal stratification.
- Fatigue refers to cyclic loading situations which, in turn, are classified as either "high cycle" fatigue, *HCF* (i.e. high frequency, low strain amplitude), or 'low cycle" fatigue, *LCF*, (i.e. low frequency, high strain amplitude) loading conditions. Cracking by fatigue can occur in both of these loading subclassifications in an " inert" environment, but corrosion fatigue (*CF*) addresses the situation where the aqueous environment adds a further component to the crack initiation and propagation process. This is especially the case for *LCF* fatigue loading situations associated with, for example, thermal mixing of cooler water with hot reactor coolant.

There is smooth transition between the cracking susceptibility of all commercially important alloy/environment systems (not just carbon and low alloy steels in water cooled reactors) and the stress/strain modes mentioned above. For this reason the overall cracking process is known as "environmentally-assisted cracking" and the following discussion emphasizes this continuity.

Table 5-1: Correlation between different submodes of *EAC*, type of loading and reactor operating conditions, Seifert, 2002.

Mechanism	**Environmentally-Assisted Cracking (*EAC*)**		
	Stress Corrosion Cracking (*SCC*)	**Strain-Induced Corrosion Cracking (*SICC*)**	**Corrosion Fatigue (*CF*)**
Type of loading	Static	Slow monotonically rising or very low-cycle	Cyclic: low-cycle, high cycle
LWR operation condition	Transient-free, steady-state power operation	Start-up/shut-down, thermal stratification	Thermal fatigue, thermal stratification, …
Characterisation of crack growth	*BWRVIP*-60 disposition lines	?	*ASME* XI, code case N-643 (*PWR*)
Characterisation of crack initiation	? (σ > YS)	Susceptibility conditions: ECP_{crit}, $d\varepsilon/dt_{crit}$, ε_{crit}	*ASME* III, F_{env}-approach

5.1 Background

Stress corrosion cracking of carbon steels in aqueous environments has been recognized for many decades, starting with cracking in boilers in the United Kingdom circa the 1870s due to the presence of excess hydroxide (Stromeyer 1909), in evaporators containing ammonium nitrate (Jones, 1921), in coal gasification plant (Welding Soc., 1951) and sour gas wells (Fraser et al., 1958) associated with sulphur-rich environments, in storage vessels containing anhydrous ammonium (Phelps & Loginow, 1962) and in chemical process plant and cathodically protected gas transmission piping associated with carbonate-bicarbonate environments, Parkins et al., 1986, Parkins & Foroulis, 1988, Parkins & Fessler, 1978. In all of these cases the temperatures have been relatively low (<150°C), but the local concentration of the "aggressive" anions has been high. These high concentrations have been associated with crevice chemistries and/or water-to-steam phase changes at leaks or in regions where boiling is localized. For instance, concentrations of 9N NaOH or 4N NH_4NO_3 are expected in the cases of caustic cracking in boilers at leaking rivet holes or of nitrate cracking in evaporators.

However, cracking of carbon steels can occur in more dilute environments, such as those found in deaerators, service water with inhibitors, or in higher purity water and wet steam associated with the higher temperatures in the reactor coolant systems in nuclear plant (Hickling & Blind, 1986) and steam turbines. In these cases the extent of cracking depends on the specific combinations of dissolved oxygen in the water, the concentration of additives, the temperature and flow rate, the stress or strain conditions, and the composition and heat treatment of the steel.

The stress corrosion cracking morphology in ductile carbon steels is generally intergranular in the lower temperature ranges, although transgranular cracking is observed in the moist CO-CO_2 environments in chemical plant, Kowaka & Nagata, 1968. The cracking morphology in the purer water chemistries at higher temperatures associated with, for example, *BWR* feedwater and condensate piping (Hickling & Blind, 1986) is also generally transgranular. However, the cracking morphology can change between the transgranular and intergranular modes in a given system with relatively minor changes in the material, environment and stressing conditions.

In all cases, as will be described in some detail momentarily, the chronology of events involves various phenomena categorized as "crack initiation" followed by sub-critical "crack propagation". The crack propagation process may arrest under given material, stress and environment conditions or it may proceed to give rise to a through-wall penetration and coolant leakage or to rapid, uncontrolled fracture of the component when the fracture toughness (K_{IC})[20] or plastic overload limit is exceeded. This latter event is rare for the ductile structural alloys, although catastrophic boiler explosions have occured in both rivetted and welded assemblies where there are stress raisers. Catastrophic failure has also been observed for the higher strength, lower fracture resistance materials such as bolting or turbine discs where the fracture toughness has been lowered due to a high yield stress or by an inadvertent heat treatment that gives rise to temper embrittlement.

[20] K_{IC} is a function of the material, the crack depth and the tensile stress

A common aspect of environmentally-assisted cracking in the various alloy/environment systems is the conjoint requirements of stress, material and environment that have to be met for a given degree of cracking susceptibility, Figure 5-1. In other words there are very specific combinations of tensile stress (applied, residual, fit-up, etc.), environment (temperature, corrosion potential, anionic concentration, etc.) and material (microstructure, yield stress, toughness, etc) that will lead to *EAC* susceptibility of a magnitude relevant to reactor operations. There is good news and bad news associated with this observation. The good news if that, because of the very specific combinations of system conditions required, the frequency of occurrences is relatively low[21], although of course, the consequence of the few occurrences of cracking that do occur can be significant. The bad news is that it is hard to define the degree of cracking susceptibility, either via experiment or analysis, due to the complicated nature of the cracking susceptibility as a function of the primary (stress, environment and material) parameters and the interactions between these parameters.

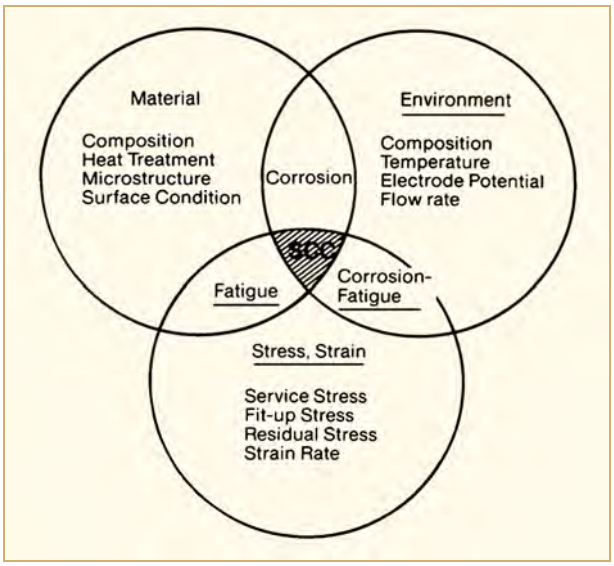

Figure 5-1: Conjoint material, stress and environment requirements for environmentally-assisted cracking, Speidel, 1984.

As indicated in Section 1, *EAC* has posed significant concerns for carbon and low alloy steels in water-cooled reactors. It should be noted at the outset that the frequency of cracking incidents has been low (compared with, for instance, cracking of austenitic alloys in both *BWR*s and *PWR*s) and has usually been associated with "upset" stress, material and/or environmental conditions. However the consequence of cracking could be significant, especially when accompanied by a transient such as a pressurized thermal shock accident in the reactor or an unusually low fracture resistance (as has happened with temper embrittlement of steam turbine disks). Such concerns, therefore, historically, have led to the following two practical questions;

1) Can we predict the time for cracking in an unclad component to progress to an extent that it would impact on structural integrity? The answer to this question requires an understanding of the various factors that govern both crack initiation and propagation, and is important for design decisions for construction of new reactors or for relicensing of existing reactors.

[21] Defined in terms of the number of welds, for instance, that exhibit cracking as a proportion of the total number of similar welds

6 References

Andrews W.K., J. Iron and Steel Institute, Vol. 203 p. 271 1965.

Andresen P.L., "*Modeling of Water and Material Chemistry Effects on Crack Tip Chemistry and Resulting Crack Growth Kinetics*" in "Proceedings of Third International Symposium on Environmental Degradation in Nuclear Power Systems–Water Reactors", Traverse City, Eds. G.J. Theus, W. Berry, The Metallurgical Society, pp. 301-314, August 30-Sept 3, 1987.

Andresen P.L., Corrosion, 44, p. 376, 1988.

Andresen P.L, Vasatis I.P and Ford F.P, "*Behaviour of Short Cracks in Stainless Steel at 288°C*", Paper 495, NACE Conference, Las Vegas, April 1990.

Andresen P.L and Ford F.P, "*Modeling and Prediction of Irradiation Assisted Cracking*", in Proceedings of Seventh International Symposium on Environmental Degradation in Nuclear Power Systems–Water Reactors, Breckenridge, Eds. R. Gold, A. McIlree, pp.893-908, 1995.

Andresen P.L., "*SCC Testing and Data Quality Consideration*", Proc. Ninth Int. Symp. on Environmental Degradation of Materials in Nuclear Power Systems – Water Reactors, AIME, pp. 411-421, 1999.

Andresen P.L., "*Irradiation Assisted Styress Corrosion Cracking*" in "Proceedings of "Mechanisms of Materials Degradation and Non-destructive Evaluation for Light Water Reactors", pp.255-300, Eds Ishino, Eyre, Kimura. Pub. INSS, Japan, May 27-29 2002.

Aria T. et al., Paper 140 NACE Corrosion Conference, 1998.

ASTM, "*Localized Corrosion-Cause of Metal Failure*", ASTM STP 516, 1972.

Atkinson J.D. and Yi J., "*The Role of Dynamic Strain Aging in the Environment Assisted Cracking Observed in Pressure Vessel Steels*", Fatigue, Fracture Eng.Mater. Struct., Vol 20, pp.1-12, 1997.

Balakrishnan P.V and Pathania R.S., "*Correlation of tube support structure corrosion studies*" in Proceedings of Third International Symposium on Environmental Degradation in Nuclear Power Systems–Water Reactors, Traverse City, Eds. G.J. Theus, W. Berry, The Metallurgical Society, pp. 489-499, August 30-Sept 3, 1987.

Bamford W.J., Rao G.V., Houtman J.L, "*Investigation of Service –Induced Degradation of Steam Generator Shell Materials*" in "Proceedings of Fifth International Symposium on Environmental Degradation in Nuclear Power Systems–Water Reactors, Monterey, Eds. D. Cubicciotti, E. Simonen, American Nuclear Society, August 25-29, 1991.

Bandyopadhyay N. and Briant C. L., Corrosion, 41, 274, 1985.

Bart A., Crockett H. M., Goyette L. F., Horowitz J. S. and Montgomery R., "*Flow accelerated corrosion – the entrance effect*", PVP2008-61185, Proceedings of PVP2008, 2008 ASME Pressure Vessels and Piping Division Conference, Chicago, Illinois, USA, July 27-31, 2008.

Baum A., "*Experimental Evaluation of Tube Support Plate Crevice Chemistry*", in "Proceedings of 10th Int. Symposium on Environmental Degradation of Materials in Nuclear Power Systems - Water Reactors", Lake Tahoe, NACE International 2001.

Beavers J.A and Pugh E.N, Met. Trans. 11A, p. 809, 1980.

Beavers J. A., Agrawal A.K. and Berry W.E., "*Corrosion Related Failures in Power Plant Condensers*", EPRI, Palo Alto, Report # NP-1468, August 1980.

Beck T.R, Corrosion 30, p.408, 1974.

Berge Ph., Ribon C., P and St Paul P., "*Effect of Hydrogen on the Corrosion of Steels in High Temperature Water*", Corrosion, 32 (No.6, June), pp.223-228, 1976.

Birnbaum H.K., "*Hydrogen Embrittlement*" in "Proceedings of First International Conference on Environmentally Assisted Cracking of Metals", Kohler Wisconsin, Eds. R. Gangloff & B. Ives, Pub. NACE, pp. 21-29, October 2-7, 1988.

Berry W.E. and Diegle R.B., "*Survey of Corrosion Product Generation, Transport and Deposition in Light Water Reactors*", EPRI NP-522 March, 1979.

Beachem C.D, Met. Trans. 3, p. 437, 1972.

Bignold G.J., Garbett K. and Woolsey I.S, "*Mechanistic Aspects of the Temperature Dependence of Erosion–Corrosion*", Proceedings of Conference "Corrosion Erosion of Steels in High Temperature Water and Wet Steam", May1982 Eds. Ph Berge, F. Kahn. Pub. Electricitie de France, May, 1982.

Bignold, C. J., de Whally, C. H., Garbett, K., Woolsey, I. S., "*Mechanistic aspects of erosion-corrosion under boiler feedwater conditions",* Proceedings of Water Chemistry of Nuclear Reactor Systems III, BNES, p. 219-226, 1983.

Billy A. F., "*Background and history of the bolting degradation or failure in nuclear plants issue*", Proceedings of EPRI seminar on Bolting Degradation or Failure in Nuclear Plants, Knoxville, November, 1983.

Bloom M.C., "*A Survey of Steel Corrosion Mechanisms Pertinent to Steam Power Generation*", Proceedings of 21st American Water Conference, 1960.

Bohni H. and Uhlig H.H., "*Environmental Factors Affecting the Critical Pitting Potential of Aluminium*", J. Electrochemical Soc. 116, p. 906, 1969.

Bohni H, "*Localized Corrosion of Passive Metals*" in "Uhligs Corrosion Handbook", Second Edition, Ed.. R. Winston Revie. Pub. John Wilety and Sons, pp.173-190, 2000.

Bohenkamp K., "*Caustic Cracking of Mild Steel", in "Stress-Corrosion Cracking and Hydrogen Embrittlement of Iron-Base Alloys*", Firminy, France, June 1973. (R.W. Staehle, J. Hochmann, R.D. McCright and J.E. Slater, Eds.), p. 374, NACE, Houston, 1977.

Bogaerts W.F., Van Haute A.A. and Brabers M.J., "*Relative Critical Potentials for Pitting Corrosion of 304 Stainless Steel, Incoloy 800 and Inconel 600 in Alkaline High Temperature Aqueous Solutions*", J. Nuclear Mat., 115, pp. 339-342, 1983.

Briant C.L., Met. Trans. 10A, p.181, 1979.

Brown B.F., Conference on, "*Localized Corrosion*", Dec 6-10, 1971 Williamsburg, Ed. B.F. Brown, J. Kruger, R.W. Staehle, Pub NACE, 1974.

Brown K.S. and Gordon G.M., "*Effects of BWR Coolant Chemistry on Propensity for IGSCC Initiation and Growth in Creviced Reactor Internals Components*", in Proceedings of Third International Symposium on Environmental Degradation in Nuclear Power Systems – Water Reactors", Eds. G.J Theus, W Berry. Published by The Metallurgical Society. ISBN 0-87339-030-X, pp.243-248 Traverse City, August 30-Sept 3, 1987.

Bruemmer G. et al., "*Beschreibung einer einhüllenden Risswachstumskurve zum Spannungsrisskorrosions-verhalten von ferritischen Reaktordurckbehälter (RDB)-Stählen unter Siedewasser (SWR)-Bedingungen*", Proc. of 28th MPA Seminar, Safety and Reliability in Energy Technology, Vol. 1, Paper No.13, pp. 13.1 – 13. 30, Stuttgart, Germany, October 10 and 11, 2002.

Bruemmer G., Hoffmann H., Huttner F., Ilg U., Wachter O., Widera M., Brozova, A. Burda J., Erben O., Ernestova M., Kysela J., Postler M. and Vsolak R., "*Investigation on Environmentally Assisted Cracking Behaviour of a Ferritic Reactor Pressure Vessel Steel under the Simultaneous Influence of Simulated BWR Coolant and Irradiation*" in "Proceedings of Eleventh International Conference on Environmental Degradation in Nuclear Power Systems– Water Reactors", Skamania Lodge, Eds. G. Was, L. Nelson, American Nuclear Society, pp.116-125, August 5-9, 2003 Stevenson, August, 2003.

Brush E.G. and Pearl W.L., "*Corrosion and Corrosion Product Release in Neutral Feedwater*", Corrosion, 28, pp.129-136, (no. 4, April), 1972.

Bulloch J.M., "*Environmental Assisted Cracking Phenomena in Reactor Pressure Vessel Steel – the Role of Manganese Sulphide Segregation*", Proc. 3rd International Symposium on Environmental Degradation of Materials in Nuclear Power Systems – Water Reactors, TMS, pp. 261 – 268, 1987.

Bussert B.W., Curran R.M. and Gould G.C., "*The Effect of Water Chemistry on the Reliability of Modern Large Steam Turbines*", J. Eng. Power 1-6, 1978.

Campbell C. A., Fyfitch S., Martin D. T., "*Boric acid corrosion of carbon and low alloy steels*", Corrosion'94, Paper 166, NACE International, 1994.

Celovsky A. et al., "*S-08; Investigation and Repair of a Cracked Feeder at Point Lepreau GS*", CANDU Maintenance Conference, 2000.

Chao C.Y., Lin Y. and MacDonald D.D., "*A Point Defect Model for Anodic Passive Films 1. Film Growth Kinetics*", J. Electrochemical Soc., 128, p.1187, 1981.

Cieslak W. and Duquette D., "*The Pit Initiation Resistance of Ferritic Stainless Steel in Chloride Environments from 80 to 260°C*" in "Proceedings of First International Symposium on Environmental Degradation in Nuclear Power Systems – Water Reactors, Myrtle Beach, August 22-25, 1983. Eds. J. Roberts, W. Berry, National Association of Corrosion Engineers, pp. 438-450, 1983.

Chexal V. K. and Horowitz J. S., "*Flow assisted corrosion in carbon steel piping; parameters and influences*", Proceedings of 4th Int. Symposium on Environmental Degradation of Materials in Nuclear Power Systems - Water Reactors, Jekyll Island, p. 9-1 to 9-12, NACE, 1990.

Chexal B., Horowitz J., Jones R., Dooley B. and Wood C., "*Flow Accelerated Corrosion in Power Plants*", EPRI Report TR-106611, June 1996.

Chopra O.K and Shack W.J., "*Effects of Light Water Reactor Coolant Environments on Fatigue Crack Initiation in Carbon & Low–Alloy Steels andAustenitic Stainless Steels*", Proceedings of The Third International Conference on Fatigue of Reactor Components, Seville, Spain, October 4–6, 2004.

Cohen P., "*Water Coolant Technology of Power Reactors*", 2nd edition American Nuclear Society 1980.

Combrade P., "*Prediction of Environmental Crack Growth in Nuclear Power Plant Components*", Final Report of EPRI Contact RP2006-1 and RP2006-8, 1990.

Combrade P. et al., "*Oxidation of Nickel Base Alloys in PWR Water; Oxide Layers and Associated Damage*" in "Proceedings of Twelfth International Conference on Environmental Degradation in Nuclear Power Systems–Water Reactors, Snowbird, Eds. L. Nelson, P.J. King, The Metallurgical Society, pp. 883-890, August 5-9, 2005.

Cooper W.E., "*The Initial Scope and Intent of the Section III Fatigue Design Procedure*" In Welding Research Council Inc Technical information from Workshop on Cyclic Life and Environmental Effects in Nuclear Applications Clearwater, Florida, January 20-21, 1992.

Cowan R.C et.al., "*The ICCGR Interlaboratory Round Robin on Slow Strain Rate SCC of PWR Forging*", in "Proceedings of Second International Atomic Energy Agency Specialists Meeting on Subcritical Crack Growth", Sendai Japan, NUREG CP-0067, pp. 181-197, May 15-17, 1985.

Cragnolino G., "*A Review of Pitting Corrosion in High Temperature Aqueous Solutions*", in "International Conference on Localized Corrosion", Pub NACE Houston Florida, 1987.

Crockett H.M., Hiranuma N., Honjin M., Horowitz, J.S., "*A comparison of FAC programs in Japan and the United States*", PVP2008-61311, Proceedings of PVP2008, 2008 ASME Pressure Vessels and Piping Division Conference, Chicago, Illinois, USA, July 27-31, 2008.

Czajkowski C.J., "*Corrosion and Stress Corrosion of Bolting Materials in Light Water Reactors*", Proceedings of 1st Int. Symposium on Environmental Degradation of Materials in Nuclear Power Systems - Water Reactors, p 192-208, Myrtle Beach, NACE, 1984.

Czajkowski C.J., "*Metallurgical Evaluation of an 18 inch Feedwater Line Failure at the Surry Unit 2 Power Station*", NUREG/CR-4868, Brookhaven Nat. Lab. March, 1987.

Daret J. and Pinard-Legry G., "*Intergranular Attack (IGA) of PWR Steam Generator Tu bing; Evaluation of Remedial Properties of Boric Acid*" in Proceedings of Third International Symposium on Environmental Degradation in Nuclear Power Systems–Water Reactors, Traverse City, Eds. G.J. Theus, W. Berry, The Metallurgical Society, pp. 517-523, August 30-Sept 3, 1987.

Davies M.J., Woolsey I.S., McGuigan J. and Renwick T., "*Erosion-corrosion in AGR boilers*", Proceedings of Chimie 2002, Avignon, France, 22-26 April, 2002.

de Kazinski F., J. Iron Steel Inst. 177, p. 85, 1954.

Dexter S.G., "*Localized Biological Corrosion*", in "Corrosion", Vol. 13, Metals Handbook, Pub. *ASM* International, pp.114-122, 1987.

Diercks D.R., Shack W.J and Muscara J., "*Overview of Steam Generator Tube Degradation and Integrity Issues*", Nuclear Engineering and Design, 194, pp.19-30, 1999.

Eason E. et al., WRC Bulletin, 404, pp. 38 – 51, 1995.

Eason E. et al., Nuclear Engineering & Design, 184, pp. 89 – 111, 1998.

Edeleanu C and Forty A.J, Philos. Mag. 5, p.1029, 1960.

Environmental Degradation Conferences:

- *Proceedings of First International Symposium on Environmental Degradation in Nuclear Power Systems – Water Reactors*, Myrtle Beach, August 22-25, 1983. Eds. J. Roberts, W. Berry, National Association of Corrosion Engineers, 1983.
- *Proceedings of Second International Symposium on Environmental Degradation Systems-Water Reactors, Monterey*, Eds. J. Roberts, J. Weeks, American Nuclear Society, September 9-12, 1985.